# TORSIONAL BEHAVIOURS AND CRACK LOCALIZATION IN PALM OIL CLINKER CONCRETE

SAFDAR KHAN

FACULTY OF ENGINEERING,
UNIVERSITY OF MALAYA
KUALA LUMPUR

2021

# TORSIONAL BEHAVIOURS AND CRACK LOCALIZATION IN PALM OIL CLINKER CONCRETE

**SAFDAR KHAN**

**DISSERTATION SUBMITTED IN FULFILMENT OF THE REQUIREMENTS FOR THE DEGREE OF MASTER OF ENGINEERING SCIENCE**

**FACULTY OF ENGINEERING**
**UNIVERSITY OF MALAYA**
**KUALA LUMPUR**

**2021**

**UNIVERSITY OF MALAYA**

**ORIGINAL LITERARY WORK DECLARATION**

Name of Candidate: SAFDAR KHAN

Matric No: KGA180038 / 17198186/1

Name of Degree: Master in Structural Engineering & Materials (Civil Engineering)

Title of Project Report: "Torsional Behaviours and Crack Localization in Palm Oil Clinker Concrete"

Field of Study: Structural Engineering & Materials (Civil Engineering)

I do solemnly and sincerely declare that:

(1) I am the sole author/writer of this Work;
(2) This Work is original;
(3) Any use of any work in which copyright exists was done by way of fair dealing and for permitted purposes and any excerpt or extract from, or reference to or reproduction of any copyrighted work has been disclosed expressly and sufficiently and the title of the Work and its authorship have been acknowledged in this Work;
(4) I do not have any actual knowledge nor do I ought reasonably to know that the making of this work constitutes an infringement of any copyrighted work;
(5) I hereby assign all and every right in the copyright to this Work to the University of Malaya ("UM"), who henceforth shall be the owner of the copyright in this Work and that any reproduction or use in any form or by any means whatsoever is prohibited without the written consent of UM having been first had and obtained;
(6) I am fully aware that if in the course of making this Work, I have infringed any copyright whether intentionally or otherwise, I may be subject to legal action or any other action as may be determined by UM.

Candidate's Signature Date:10-06-2021

Subscribed and solemnly declared before,

Witness's Signature Date:

Name:

Designation:

## ABSTRACT

The utilization of a Palm oil clinker for the production of sustainable lightweight concrete has environmental, economic, and social benefits. This study presents the investigation of the torsional behavior and localization of cracks in concrete at different substitution levels of POC coarse aggregate with granite. The DOE method was used for the design of the control mix, and all other mixes were prepared with the substitution of granite with the increasing amounts of POC at replacement levels of 20%, 40%, 60%, 80%, and 100%. The maximum reduction in the hard density, compression strength, splitting tensile strength, and flexural strength was 18.80%, 37.25%, 30.94%, and 15%, but an increment in water absorption of 1.78 times higher than the POC0 mix at the full substitution of POC with granite. The impact energies (first and failure cracks) at 60% and 100% incorporation of POC were approximately 4 and 1.60 times higher than control mix. The torque at initial and ultimate cracks were decreased by increasing the substitution levels of POC coarse aggregate. The POC100 had 1.64, and 2 times lower initial torsional stiffness, and torsional toughness as compared to NWC. The initial crack has happened almost in the range of 14-25% of the ultimate crack. The rise in the AE activities, when the initial, and ultimate cracks have developed accompanied by a dropped in the torque-twist curve, after the ultimate torque. The initial crack, ultimate crack, initial, and ultimate torque have been investigated by using the acoustic emission parameters such as absolute energy, and cumulative signal strength.



**Keywords:** Acoustic emission parameters; Crack mapping; Mechanical properties; Palm oil clinker; Torsional behavior.

## ABSTRAK

Penggunaan klinker minyak sawit untuk pengeluaran konkrit ringan lestari mempunyai manfaat alam sekitar, ekonomi, dan sosial. Kajian ini menyajikan penyelidikan tingkah laku kilasan dan penyetempatan retakan pada konkrit pada tahap penggantian agregat kasar POC dengan granit. Kaedah DOE digunakan untuk reka bentuk campuran kawalan, dan semua campuran lain disiapkan dengan penggantian granit dengan peningkatan jumlah POC pada tahap penggantian 20%, 40%, 60%, 80%, dan 100%. Pengurangan maksimum ketumpatan keras, kekuatan mampatan, kekuatan tegangan pemisah, dan kekuatan lenturan adalah 18.80%, 37.25%, 30.94%, dan 15%, tetapi peningkatan penyerapan air 1.78 kali lebih tinggi daripada campuran POC0 pada penggantian penuh POC dengan granit. Tenaga impak (retak pertama dan kegagalan) pada 60% dan 100% penggabungan POC adalah kira-kira 4 dan 1.60 kali lebih tinggi daripada campuran kawalan. Tork pada retakan awal dan akhir diturunkan dengan meningkatkan tahap penggantian agregat kasar POC. POC100 mempunyai kekakuan kilasan awal 1.64, dan 2 kali lebih rendah, dan ketangguhan kilasan berbanding NWC. Keretakan awal telah berlaku hampir dalam lingkungan 14-25% dari retakan utama. Kenaikan aktiviti AE, ketika retakan awal dan akhir telah berkembang disertai dengan penurunan pada lengkung tork-twist, setelah tork utama. Keretakan awal, retak utama, tork awal, dan akhir telah disiasat dengan menggunakan parameter pelepasan akustik seperti tenaga mutlak, dan kekuatan isyarat kumulatif.



**Kata kunci:** Parameter pelepasan akustik; Pemetaan retak; Sifat mekanikal; Klinker minyak sawit; Tingkah laku kilas.

## TABLE OF CONTENTS

# LIST OF FIGURES

# LIST OF TABLES

## LIST OF ABBREVIATIONS AND SYMBOLS

| | | |
|---|---|---|
| AE | : | Acoustic emission |
| AIV | : | Aggregate impact value |
| ASTM | : | American society for testing and materials |
| BS | : | British code |
| CS | : | Coconut shell |
| CSS | : | Cumulative signal strength |
| Dia. | : | Diameter |
| ELE | : | Engineering laboratory equipment |
| ITZ | : | Interfacial transition zone |
| LWA | : | Lightweight aggregate |
| LWC | : | Lightweight concrete |
| NWC | : | Normal weight concrete |
| OPBC | : | Oil palm boiler clinker |
| OPC | : | Ordinary Portland cement |
| OPKS | : | Oil palm kernel shell |
| OPS | : | Oil palm shell |
| OPSC | : | Oil palm shell concrete |
| OPSGPC | : | Oil palm shell geopolymer concrete |
| POFA | : | Palm oil fuel ash |
| POC | : | Palm oil clinker |
| POCP | : | Palm oil clinker powder |
| POCC | : | Palm oil clinker concrete |
| PSCC | : | Palm Shell and Clinker Concrete |
| SEITS | : | Strain energy impact test system |

| | | |
|---|---|---|
| SHM | : | Structural health monitoring |
| SLWC | : | Structural lightweight concrete |
| SSD | : | Saturated surface dry |
| RA | : | Recycled aggregate |
| UPV | : | Ultrasonic pulse velocity |
| % | : | Percentage |
| mm | : | Millimeter |
| $m^3$ | : | Cubic meter |
| N | : | Newton |
| kg | : | Kilogram |
| µm | : | Micrometer |
| w/c | : | Water cement ratio |

# CHAPTER 1: INTRODUCTION

## 1.1 Background

The recycling of waste materials has gained the attention of researchers all over the world because of the growing need for sustainable development (Aslam, Shafigh, & Jumaat, 2016). The interest in recycling waste has been driven by the need to reduce waste generated by rapid growth in industrial and technological sectors. One of the possible uses of waste materials in the industry of construction is as alternatives to normal-weight aggregate in concrete production (Gayana & Chandar, 2018; Ibrahim & Razak, 2016; Mohammed, Foo, Hossain, & Abdullahi, 2013; Thomas, Thaickavil, & Abraham, 2018). The recycling of waste materials in the concrete production results in cost savings, in addition to weight reductions (Abutaha, Razak, Ibrahim, & Ghayeb, 2018; Abutaha, Razak, & Kanadasan, 2016; Ahmmad et al., 2016; M. Mannan & Ganapathy, 2004). In terms of environmental benefits, the use of waste materials as a replacement to natural aggregates helps in the preservation of natural resources and reduces solid wastes (Shafigh, Mahmud, & Jumaat, 2012; Sharath, Gayana, Reddy, & Chandar, 2019; Suman & Rajasekaran, 2016) and $CO_2$ emission (Ibrahim, Razak, & Abutaha, 2017).

In a tropical country like Malaysia, the incorporation of agricultural waste in concrete is studied extensively since 1984 (Ahmmad et al., 2016). Malaysia is the second-largest palm oil producer in the world, accounting for more than half of the global palm oil production. The palm oil industry generates a large amount of agricultural waste products, which are usually burned in palm oil mills to produce the steam required for the oil extraction process. Such incineration, in turn, generates solid waste byproducts that contain significant amounts of Palm Oil Clinker (POC). The low commercial value of POC and its demands of landfill space and dumping sites (Abutaha et al., 2016; Jumaat, Alengaram, Ahmmad, Bahri, & Islam, 2015), necessitate recycling of this waste product.

POC is porous with large voids, broken edges, and irregular shapes, as seen in Figure 1.1(a) and is often used as an aggregate to replace conventional crushed granite in concrete (Abutaha et al., 2018; Ibrahim & Razak, 2016; Kanadasan & Razak, 2015). The POC is often crushed to the required size and to added as an aggregate for the POC concrete (POCC) production (Mohammed et al., 2013).

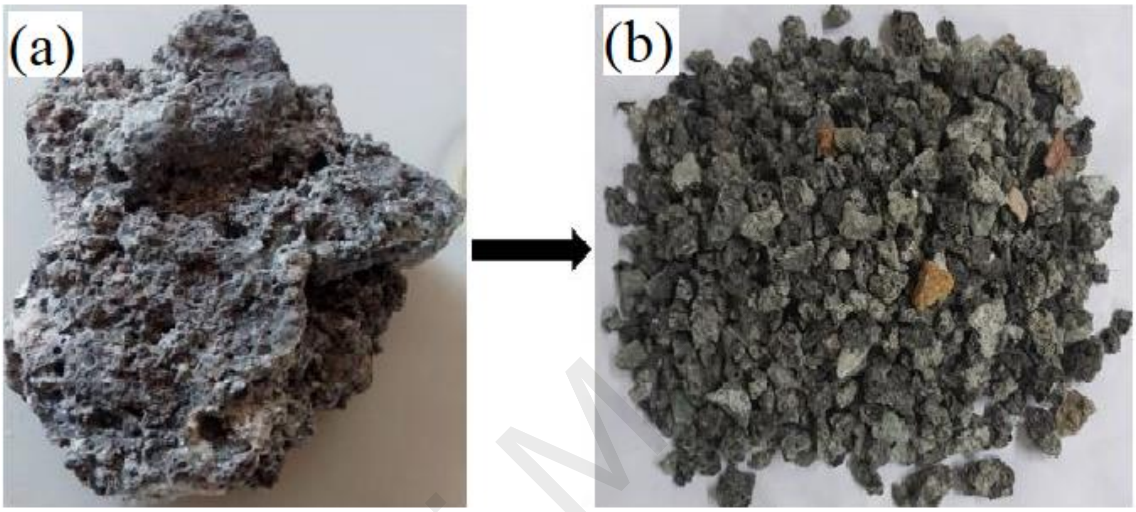


**Figure 1.1: (a) Chunk, and (b) grounded palm oil clinker (POC)**

All studies on POCC have hitherto focused on their mechanical properties and long-term behavior (Abutaha, Abdul Razak, & Ibrahim, 2017; Abutaha et al., 2018; Abutaha et al., 2016; Ahmmad et al., 2017; Ahmmad et al., 2016; Huda, Jumaat, Islam, Obaydullah, & Hosen, 2017; Ibrahim & Razak, 2016; Ibrahim et al., 2017; Jumaat et al., 2015; Karim, Chowdhury, Zabed, & Saidur, 2018; Mohammed et al., 2013).

Few studies have dealt with the torsional behavior of concrete containing lightweight aggregates (George & Sofi, 2018; Yap, Alengaram, Jumaat, & Khaw, 2016; Yap, Khaw, Alengaram, & Jumaat, 2015), and there have been, to the best of our knowledge, no studies on the torsional behavior of POCC. It is important to know about the torsional properties of POCC because torsion-loaded members made using such concrete may experience torsional cracking before or with flexural or shear failure, as the torsional strength is highly dependent on the tensile strength, which is the weakest component in brittle concrete. It is perhaps more important to study torsional failure of the torsional-loaded concrete member than flexural or shear failure because torsional failure precedes flexural failure (George & Sofi, 2017). The lower density of the LWC has the allow the structure or member for the great design flexibility and economic benefit, because of reduction in self-weight of the concrete member and structure (Yap, Bu, Alengaram, Mo, & Jumaat, 2014). The LWC is commonly used in slabs and joists of high rise buildings and bridge decks of highway bridges as well as offshore and marine structures (Ahmmad, Jumaat, Bahri, & Islam, 2014; Jumaat et al., 2015) and also used in pavement, parking places etc. The evaluation of the initial crack and ultimate crack formation is essential to predict structural integrity and performance, particularly in concrete with low tensile strengths.

It is also necessary to evaluate the location of the crack, fracture, and their impact on the condition of the structure as part of service life assessment. For this, it is essential to understand the methods used to detect the cracks, deterioration process, and to monitor the progress of damage and cracks within the entire structure. Of the available methods, the acoustic emission (AE) method is capable detecting and assessing fracture or damage by capturing the release of energy and signals during crack formation (Qian, Farnam, & Weiss, 2014). The AE method also allows for the detection of cracks due to mechanical loading, freeze-thaw cycle, etc. during which, cracks are initiated and propagated. It is a non-invasive, passive, non-destructive, and a type of elastic wave method for the detection of crack initiation and propagation, materials degradation and corrosion, and plastic deformation. It is a better supportive method than elastic wave methods such as impact echo (IE) method, ultrasonic pulse velocity method (UPV) (Zaki, Chai, Aggelis, & Alver, 2015). Earlier studies (Landis & Baillon, 2002; Qian et al., 2014) have used the non-invasive, and real-time AE method for the investigation of the fracture process in concrete. It has been shown that this method can localize cracks, test entire structures, and also provide information about the materials' responses to applied stress (Mazal, Vlasic, & Koula, 2015).

## 1.2 Problem statements

Recently many innovative and researchers have given much attention to the utilization of waste material in the industry of construction. The reduction of waste material and their byproducts generate from the rapid growth of the industrial and technological sectors is very necessary to reduce environmental pollution, preservative of natural resources, and economic benefits to achieving sustainability. Different types of waste materials that have been substituted into construction include seashell byproduct, ceramic sanitary waste, wood chippings, crumb rubber, oil palm shell (OPS), palm oil fuel ash (POFA), POC and others (Ahmmad et al., 2016; Halicka, Ogrodnik, & Zegardlo, 2013; Ibrahim & Razak, 2016; Mohammed et al., 2013) but our research on the use of agriculture waste materials in the sustainable concrete production. Tropical countries like Malaysia produced a higher amount of agricultural waste materials and their byproducts such as OPS, OPBC, and POC. Therefore, to use the POC aggregate as a coarse aggregate instead of granite in the production of green concrete to secure the environment, preservation of natural resources, economic benefits, weight reduction of member or structure, and to allow for great flexibility because of the lower bulk density.

Besides, many literature reviews available on the mechanical properties and long-term behaviors of palm oil concrete but none of the literature reviews are available on the torsional behavior of concrete based on the POC aggregates. The investigation of the torsional behavior of POC concrete members is very essential because of the lower torsional strength of the concrete and it depends on the tensile strength of the concrete which is the weakest component of the brittle concrete. The concrete member has resulted in torsional failure before as even the flexural or shear failure when member subjected to the torsional loading.

However, the main problem of this study is the investigation of crack propagation, initial, and ultimate torsional cracks of the concrete member by using the relevant method. For this, it is very important to know the methods that should detect the cracks, deterioration process, and capable to monitor the progress of damage, and cracks within the entire structure in the real-time application of loading. The acoustic emission is the best choice for relying on the analysis of the active destructive process (Świt, 2018). Therefore, the acoustic emission method is very sensible for the detection of cracks, fractures, damage, and also the investigation of the torsional failure of concrete.

## 1.3 Objectives

The objectives of this study are listed below.

1. Testing and analyzing of physical properties of coarse aggregates (granite and palm oil clinker) and fine aggregates.
2. To assess the mechanical properties of concrete by replacing crushed granite with different POC replacements.
3. To evaluate the torsional behavior including cracking, and ultimate torque and their corresponding twist, initial torsional stiffness, initial and ultimate torsional toughness of POC concrete at various substitution proportions of POC coarse aggregate.
4. To investigate the torsional crack localization in palm oil clinker concrete by using the parameters of the AE method.

## 1.4 Scopes of work

The scopes of this research are separated into two main parts (i) Testing of physical properties of aggregates, mixing, and casting of concrete specimen and (ii) Testing and analysis of the hardened properties, and investigation of the torsional behavior and torsional crack localization.

The first part is corresponding to the Objective 1, at which the physical properties such as bulk density, aggregate impact value (AIV), specific gravity, and water absorption of coarse aggregate (POC and granite), and fine aggregate (sand) tests have been performed to get the information to help for designing a correct concrete mixture. Based on physical properties, the concrete mixture was designed for the investigation of hardened properties and the torsional test of the concrete. After the testing of physical properties of aggregates, the concrete will be prepared by mixing the materials according to the required proportion, and standards, and casting of concrete with the incorporation of POC coarse aggregate at 0%, 20%, 40%, 60%, 80%, and 100% with granite. The replacements level of coarse aggregates in this research was selected on the previous papers (Abutaha et al., 2017; Ibrahim & Razak, 2016; Jumaat et al., 2015) that the maximum replacements can be go up to 100%, with 20% intervals in order to study the effects of replacement levels of 0, 20, 40, 60, 80 and 100%.. The resulting concrete will be molded into cubes, cylinders, and prisms according to the required specification of tests.

While Objectives 2, 3, and 4 are covered by part (ii), at which all the mechanical properties such as hardened density, compression strength, water absorption, UPV value, flexural strength, splitting tensile strength, and impact test were tested at 28 days of curing. The 28 days of curing is generally used for conventional concrete including POC concrete (Kabir et al., 2017; Mohammed et al., 2013) and thus the 28-day testing results can be used to be compared with other studies. All the tested properties data were analyzed and based on this data the torsional behavior and cracking resistance of concrete were investigated. All testing and sizes of all specimens for all tests are chosen according to the specified standards. The investigation and comparing of the torsional behavior and cracking resistance of specimens of 500 mm × 100 mm × 100 mm by using the acoustic emission method. The data analyzed from the torsion deflection curve of the torsion machine compared with the data analyzed from the AE method to obtain the torsional behaviours such as initial torsional stiffness, ultimate torsional toughness, first, and ultimate cracks, and the torque, and their corresponding twists of the POCC. The graphs of AE parameters named absolute energy and CSS versus twist were compared with the torque-twist curves to identify and localization of initial crack, propagation of the crack, ultimate crack caused by torsion loading.

## 1.5 Organization of thesis

This section explains the layout of the thesis, which contains five chapters that are an introduction, literature review, methodology, results, and the last chapter is the conclusions, and a list of figures, tables, abbreviations, and symbols. Each chapter and portion of the thesis cover different components of the study. A summary of all the chapters is mentioned as follows.

- Chapter 1 Introduction; that covers the background of research, problem statements, objectives, the scope of work, and the layout of the thesis related to the research.
- Chapter 2 Literature review; that contains the literature about LWAC, previous studies about agriculture waste materials, the performance of concrete with substitution of POC aggregates, torsional behavior, localization, and identification of cracks by using the AE method.
- Chapter 3 Methodology; that describes the tests for material properties, methods, and specifications used for the hardened properties of concrete, and torsional behavior by using the acoustic emission method.

- Chapter 4 Results and discussion; that explains the hardened properties, impact test, torsional behavior, localization of cracks of concrete at different replacement levels of POC by using the AE method.
- Chapter 5 presents the conclusions drawn in this research, and the recommendations for future research which can be conducted to improve the understanding on torsional behaviours of lightweight concrete.

# CHAPTER 2: LITERATURE REVIEW

## 2.1 Lightweight concrete

The lightweight concrete (LWC) has been utilized from ancient's times and in the most interesting fields of research because of the many advantages and benefits (Aslam, Shafigh, Nomeli, & Jumaat, 2017). In the past history, different types of natural and manufactured LWAs, such as foamed slag, diatomite, pumice, volcanic cinders, scoria, tuff, expanded clay, shale, slate, perlite and vermiculite and materials that occur as industrial by-products, such as sintered pulverized-fuel ash, sintered slate and colliery waste, and foamed or expanded blast-furnace slag have been used as construction materials for the production of LWAC (Aslam, Shafigh, & Jumaat, 2016). They drastically change in the field of concrete technology. The development of the LWC by using the waste material has a sustainable improvement in the performance of the concrete, working conditions, construction cost, and environment. The advantages of the usage of the LWC has a reduction in self-weight of the foundation, structure, frost and fire resistance, heat insulation, and increased seismic damping (Abutaha et al., 2016; Aslam, Shafigh, & Jumaat, 2016). The usage of LWAC has a benefit to saving of 10% to 20% of the total cost equivalent to the normal weight concrete (NWC) because of the lower density of the concrete and allows for the smaller structural member (Jumaat, Alengaram, & Mahmud, 2009).

The main parameter of concrete is the density that categories the concrete as a normal weight concrete or lightweight concrete. The LWC is the concrete that has a lower density as compared to the NWC. According to the BS standard (BS EN 206:2013, 2014), the concrete has categories according to their oven-dried densities. The oven-dried density for the normal weight concrete has comes in the range of 2000 kg/m$^3$ to 2600 kg/m$^3$ while the oven-dried density for LWC has not less than 800 kg/m$^3$ and not more than 2000 kg/m$^3$. The oven-dry density of concrete has more than 2600 kg/m$^3$ is called heavy concrete.

According to ASTM: C330 the minimum compressive strength of structural lightweight concrete has 17 N/mm$^2$ and the air dried-density has normally not more than 2000 kg/m$^3$ while according to the Canadian Standards (CSA), the minimum 28 days compressive strength of lightweight concrete has not less than 20 MPa and air dry-density is not more than 1850 kg/m$^3$ (Mohammed et al., 2013).

The advantage of a lower density of the LWC has allowed the structure or member for the great design flexibility and economic benefit because of the reduction in the self-weight of the concrete member and structure (Yap et al., 2014). The commonly utilization of LWC has in joists and slabs of high rise buildings and bridge decks of highway bridges as well as marine structures (Ahmmad et al., 2014; Jumaat et al., 2015) and also used in pavement, parking places, etc.

The lightweight concrete can be divided into three main categories according to their way of creation (Düzgün, Gül, & Aydin, 2005; Nazreen et al., 2018).

- Aerated, gas or cellular: in this method, the gas bubbles are inserted in the concrete with help of chemical admixture and mechanical forming to creating like cellular structure therefore it is also called gas or cellular concrete.
- No fine: the method in which the fines particles are omitted from the total portion of the concrete aggregates.
- Lightweight aggregate concrete: the concrete which is produced by using the lightweight aggregate either natural, artificial, or agricultural, and the produced concrete is porous with low density.

The most popular and important method used for the production of LWC is lightweight aggregate concrete (Düzgün et al., 2005). Various types of LWA were used for the LWAC production from ancient times and the usage of the LWC is increasing day by day because of the various advantages and benefits of lightweight aggregate. Besides the artificial or natural lightweight aggregate, the agricultural material is also used in the LWAC production.

## 2.2 Lightweight aggregate

In many developing countries the use of waste material as an alternative material for construction because of the high-cost raw material and deficiency of natural resources as well as increasing in the population of the world to fulfill the demands of the people for their shelter. When these waste materials are properly processed may be effective as a construction material as (LWA) for the manufacturing of concrete and also fulfills the design specification. LWA is the aggregates that have low bulk density and specific gravity as compared to the normal weight aggregate used for the production of concrete. The LWA has been divided into two main categories that are natural aggregates and manufactured aggregates (Aslam, Shafigh, & Jumaat, 2016; Hamada, Jokhio, et al., 2019). The natural LWA mainly contains are diatomite, pumice, cinders, scoria, volcanic and tuff. While the manufactured LWA is further subdivided into two groups industrial by-products and naturally occurring materials that will require further processing. The main industrial by-products are the sintered slate, ash, foamed blast furnace slag, and colliery waste while the naturally occurring material that required further processing are expanded clay, shale, slate, perlite, and vermiculite. The ceramic waste material may be used as a building material especially as raw material for concrete production (Halicka et al., 2013). The higher amount of internal and external voids of LWA have a lower coefficient of thermal expansion, higher better tensile strain capacity, strength/weight ratio, and higher sound and heat insulation. An alternative lightweight aggregate besides natural and artificial LWA in tropical regimes or countries are the agricultural LWA and their byproducts that have from the industry of palm oil such as OPS, OPKS, coconut shell, and POC that has been used in the manufacturing of concrete. The usage of agriculture wastes as construction material have double advantages that they have a means of disposal of waste materials and also a low cost of construction cost (M. Mannan & Ganapathy, 2004). These light weight aggregates have utilized as a replacement or potential materials in the industry of construction for the production of concrete.

## 2.3 Agriculture waste material for the production of concrete

Recently many innovative and researcher has given much attention towards the usage of waste material in the industry of construction. The reduction of waste material and their byproducts generate from the rapid growth of the technological and industrial sectors is very necessary to decrease environmental pollution, preservative of natural resources, and economic benefits to achieving sustainability. Various types of waste materials that have generated from the agriculture sector have been substituted into the industry of construction include POFA, OPS, POC, crumb rubber, seashell byproduct, and ceramic sanitary waste, etc. (Ahmmad et al., 2016; Halicka et al., 2013; Ibrahim & Razak, 2016; Mohammed et al., 2013). The waste materials would be utilized as construction material in the manufacturing of concrete (Ahmmad et al., 2016; Ibrahim & Razak, 2016; Mohammed et al., 2013). The advantage of waste materials and their by-products used as an LWA in the concrete production is more economical because of low cost in addition to lower weight (Abutaha et al., 2018; Abutaha et al., 2016; Ahmmad et al., 2016; M. Mannan & Ganapathy, 2004). Environmentally friendly because of the preservation of natural resources, and reduction in solid wastes (Abutaha et al., 2016; M. Mannan & Ganapathy, 2004; Shafigh et al., 2012), and less emission of $CO_2$ (Ibrahim et al., 2017) as compared to natural aggregate.

In tropical countries like Malaysia, the use of agricultural waste in the concrete production is more well-known and abundant because Malaysia is the second-largest country in the world for the palm oil producing due to which produced a large amount of agricultural waste and their byproducts like OPS, POC, OPBC, and OPKS, etc. These agricultural waste and their byproducts are mostly produced by the palm oil industry which was about 3.13 million tons of palm shell as waste (M. A. Mannan & Ganapathy, 2002), 2.66 million tonnes of solid waste (Abutaha et al., 2016), and 4 million tons of OPKS (Alengaram, Al Muhit, & bin Jumaat, 2013) annually. In developing countries like Malaysia, agriculture waste material and its byproducts have a suitable replacement for the production of lightweight concrete (Alsubari, Shafigh, Ibrahim, Alnahhal, & Jumaat, 2018; M. Mannan & Ganapathy, 2004). The agricultural wastes such as oil palm shell (OPS) (M. Mannan & Ganapathy, 2004; Shafigh et al., 2012), oil palm kernel shell (OPKS) (Alengaram et al., 2013), coconut shell (George & Sofi, 2018; Gunasekaran, Annadurai, & Kumar, 2013), and palm oil clinker (POC) (Abutaha et al., 2018; Ibrahim & Razak, 2016; Kanadasan & Razak, 2015) have been substituted as an aggregate in concrete instead of granite. The palm oil solid wastes are mostly contained OPS and POC (Ahmmad et al., 2016).

## 2.4 Palm oil clinker

Malaysia is the largest palm oil producer country in the world after Indonesia for the palm oil production and exports palm oil to the world more than half of the world (Jumaat et al., 2015). As a result of the significant amount of palm waste and their byproducts are generated from the milling process that would contribute to the nation's pollution problems. The wastes material that arises from the industries of palm oil is OPS, palm oil fibers, empty fruit bunches, and POFA (Ahmmad et al., 2016). The palm oil industry needed the steam for palm oil production as a result of incineration the by-products of palm oil wastes are produced. The byproducts obtained from the incineration process of the waste material is palm oil clinker (Mohammed, Al-Ganad, & Abdullahi, 2011). POC is mostly porous in nature, large voids, broken edges, irregular shape, and mostly available in large chunks of size range 100 to 300 mm from the burning of the palm oil fiber and palm oil shell at the proportion of 70:30 (Ahmmad et al., 2016; Ibrahim et al., 2017). The chunk and coarse form of the POC waste are also shown in Figure 1.1. Instead of disposing of POC to the environment due to low commercial value and abundant in large quantity (Abutaha et al., 2016; Jumaat et al., 2015), it is very best option for the management of waste to crush into the required size and utilized as aggregate for the POCC production to decreased the solid waste pollution, cost, preservation of natural aggregates, and make worthy because POC is friendly-environmentally, economical, and suitable construction material (Abutaha et al., 2018; Abutaha et al., 2016; Ahmmad et al., 2016; Ibrahim & Razak, 2016).

### 2.4.1 Physical properties of POC aggregate

#### 2.4.1.1 Shape, texture, and chemical composition

The color of POC aggregate has different because of the heating in the furnace and the waste materials source. The color range of POC aggregate has from grey to light black and obtained from the milling process in a boulder form. The chunk or boulder form of the POC waste has a process by crushing machines to get the required size. After the processing of the POC waste then it is been used in the production of concrete as coarse or fine aggregates either as a full or partial substitution with natural aggregates. The POC aggregate that passes through a 5 mm sieve is called fine aggregate while for coarse aggregate the POC aggregate passes through 14 mm and is retained on the 5 mm sieve (Mohammed, Foo, & Abdullahi, 2014). The POC aggregates have a rough, porous surface, and irregular texture and particle shape of POC coarse aggregate are shown in Figure 1.1(b). The edges of the POC are broken and spiky. The elements or the chemical oxide composition of POC aggregates with the percentage and the occurrence of oxides or elements in the POC waste is seen in Table 2.1.

**Table 2.1: Chemical compositions of POC waste and the percentage of oxides (Ahmmad et al., 2014)**

| Elements (as Oxides) | composition (%) |
|---|---|
| Silica ($SiO_2$) | 59.63 |
| Potassium($K_2O$) | 11.66 |
| Calcium (as CaO) | 8.16 |
| Phosphorus (as $P_2O_5$) | 5.37 |
| Magnesium (as MgO) | 5.01 |
| Iron (as $Fe_2O_3$) | 4.62 |
| Aluminum (as Al2O3) | 3.7 |
| Sulfur (as $SO_3$) | 0.73 |
| Sodium (as $Na_2O$) | 0.32 |
| Titanium (as $TiO_2$) | 0.22 |
| Others | 0.58 |

#### 2.4.1.2 Bulk density and specific gravity

The unit weight and specific gravity of POC aggregate have always lower than normal aggregate because of the void's nature of the POC aggregates. The specific gravity and bulk density have highly dependent on the voids of the aggregate. The Specific gravity of POC coarse aggregate has 1.73 with an aggregate size of 5-14 mm while bulk density has 732 kg/m$^3$ (Abutaha et al., 2016). The low bulk density of POC coarse aggregate has around 48% lighter than NWA. The bulk density of POC has 40-45% lower than conventional coarse aggregate (Hamada, Jokhio, et al., 2019). Thus the resulting concrete has reduced the self-weight of the structure and significant savings in the total cost of the construction (Mohammed et al., 2013). The bulk density and specific gravity of POC with various aggregate sizes from the previous studies are seen in Table 2.2.

**Table 2.2: Physical properties of POC coarse aggregate**

| **Properties** | **POC coarse aggregate** | |
|---|---|---|
| Aggregate size (mm) | 4.75-10 (Abutaha et al., 2018) | 5-15 (Fuad Abutaha, Hashim Abdul Razak, & Kanadasan, 2016) |
| Specific gravity | 1.81 | 1.73 |
| Bulk density (kg/m$^3$) | 732 | 732 |
| Water absorption at 24 h (%) | 4.35 | 3±2 |
| Aggregate crushing Value (%) | 56.44 | 56.44 |

#### 2.4.1.3 Water absorption

The water absorption of LWA had higher than NWA. A large amount of water has absorbed by POC aggregates as compared to crushed granite or NWA because of the higher inner and surface void of the POC is seen in Figure 1.1. The water absorption of coarse POC aggregate with the specific size is given in Table 2.2 reported from the previous studies. The water absorption for coarse POC aggregate has in the range of 4.7% to 26.5% (Hamada, Jokhio, et al., 2019). The higher water absorption of POC coarse aggregate has advantageous to the hardened concrete during the early stages of the concrete. Because the void's nature of the lightweight aggregate concrete has less sensitivity to the poor curing at the early stage as compared to NWC is because of the supply of internal store of water in the voids of the LWA (Mohammed et al., 2013).

#### 2.4.1.4 Aggregate impact value

The aggregate impact value (AIV) is essential to determine the aggregate capacity to resist the sudden load or shock. The POC coarse aggregate has lower resistance to the sudden shock or load as compared to NWA. The POC coarse aggregate has a 34% higher AIV as compared to the crushed granite (Mohammed et al., 2014; Mohammed et al., 2013). The higher AIV of POC coarse aggregate has caused because of the porous and angular edges of aggregates due to which reduction in the crushing strength of POC as compared to granite.

## 2.5 Mechanical properties of POC concrete

### 2.5.1 Hardened density

The hardened density is defined as the weight over the concrete volume. The weight of concrete is the basic parameter that decided to make a structure economical. The weight of the concrete based on LWA has always lower than traditional NWC due to this LWA based concrete has more economic and higher efficiency (Aslam, Shafigh, Nomeli, et al., 2017). The density is the main parameter for deciding the classification of concrete. Based on density, the POCC had classified as a structural LWC with an air-dried density of less than 1850 kg/m$^3$ (Mohammed et al., 2013). From the previous research (Mohammed et al., 2014), that the air-dry density of POCC had 16% less than NWC and the range of POCC was between 1818.24 kg/m$^3$ to 1845.62 kg/m$^3$ and comes LWC category which is less than 2000 kg/m$^3$, and NWC (2200 kg/m$^3$). The hardened density of POCC has lower as compared to NWC because of the lower bulk density and voids nature of the POC. The density of POCC had 28% lower than NWC at the full replacement of granite with POC (Ibrahim & Razak, 2016). The 28 days hardened density of concrete had reduced of 15% at 100% substitution of POC coarse aggregate with crushed granite.

### 2.5.2 Compressive strength

The commonly used parameter for defining the excellence and perfectness of concrete is the compressive strength. According to ASTM:330 the minimum requirement of the compressive strength for structural LWC has 17 $N/mm^2$. Based on test results obtained from the previous research that the compressive strength range between 25.5 to 42.56 $N/mm^2$ which had approximately 16% higher than the minimum requirement of the compressive strength for LWC (Mohammed et al., 2014). The compressive strength of concrete shows inversely proportional relation to the replacement levels of POC coarse aggregate because of the porous nature and irregular structure of POC coarse aggregate to reduce the bearing capacity of the concrete. The maximum reduction in compressive strength of POCC had 30% as compared to NWC because of the low aggregate crushing value of POC and the targeted mean strength of Grade 40 concrete was reduced to the Grade 25 concrete at the full substitution of POC aggregate with granite (Abutaha et al., 2016). The compressive strength of POCC was increased by up to 30% by the addition of POC powder up to 15% (Ahmmad et al., 2017). The direct replacement of coarse POC aggregate had reduced the compressive strength of high strength POCC at all ages as compared to normal concrete. The maximum reduction in the compressive strength of high strength POCC had 40% as compared to the control mix at full replacement level of POC coarse aggregate with granite (Abutaha et al., 2018). Further research said that the compressive strength of POCC had slightly increased in the range of 0-13% by the addition of POC powder. The compressive strength of self-compacting (SC) POC-based concrete had reduced by increasing the substitution levels of POC coarse aggregate. The maximum strength achieved at 100% substitution level of POC coarse aggregate had 68% of the control mix (Kanadasan & Razak, 2014).

### 2.5.3 Water absorption

Water absorption of the concrete is highly dependent on the surface and internal pores of the aggregate and the aggregate with a higher number of pores may be a higher amount of water absorption. Water absorption is an important factor for the determination of the durability index of the concrete. The water absorption of concrete based on LWA has higher as compared to the NWAC because LWA has higher porosity as compared to NWA (Ahmmad et al., 2017; Khankhaje, Salim, Mirza, Hussin, & Rafieizonooz, 2016; Topçu & Uygunoğlu, 2010). Therefore the water absorption of POCC has been increased by increasing the incorporation of POC with granite, because of POC possess high water absorption than granite (Aslam, Shafigh, & Jumaat, 2016). From the previous research that the water absorption of concrete at the full substitution of POC coarse aggregate with granite had 34% higher than the control mix because of the difference in the water absorption of POC and granite (Hamada, Yahaya, Muthusamy, Jokhio, & Humada, 2019). The water absorption of POCC had reduced by the incorporation of POC powder as compared to concrete containing POC coarse aggregate. The water absorption difference between high strength POC (HPOC) concrete and NWC had in the range 1.35-3.15% while HPOC concrete with the incorporation of POC powder had the difference in the water absorption with control mix of 1.35-2.30% because of the difference of porosity of POC aggregates and granite (Abutaha et al., 2018). The good quality concrete have water absorption less than 10% of its mass while high-quality concrete is usually less than 5% (Hamada, Jokhio, et al., 2019).

### 2.5.4 Ultrasonic pulse velocity

The ultrasonic pulse velocity test is non-destructive and the pulse velocity test is used for the determination of compactness or density, uniformity, and relative quality of the concrete. This method is used for the indication of the presence of voids, spaces, cracks, depth of cracks inside the concrete, and evaluating the effectiveness for the repair of cracks (Hwang, Bui, Lin, & Lo, 2012). The UPV is determined by the time required for an ultrasonic pulse during the initial onset on one side and a reception on the other side is measured electronically (Ahmmad et al., 2017). The lower UPV value of concrete shows that the concrete has less dense and of lower quality because of the presence of pores or cracks due to which pulse is not passing well. The UPV value of concrete based on LWA has lower than conventional concrete because of higher porosity nature of the LWA as compared to NWA (Hwang et al., 2012). The pulse rate transmitting through POCC was lower than the control mix because of higher inner and surface voids of POC aggregate as compared to crushed granite due to which the transmitting of pulse slow through these voids lies in their path. The UPV value was decreased by increasing the substitution levels of POC with granite but the UPV value of POCC is situated in the range of good concrete. The concrete had classified according to its UPV values range as excellent, very good, good, poor, and very poor when the UPV values in the range of 4.5 km/s or above, 3.5-4.5 km/s, 3.0-3.5 km/s, 2.0-3.0 km/s, and below 2.0 km/s, respectively (Kabir et al., 2017). From the previous study based on test results that 28 days UPV value for POCC was in the range between 4.4 and 5.2 km/sec at different replacement levels of POC with granite. Further research said that the reduction in the UPV values for HPOC and HPOCF concrete mix were in the range 3-13% and 1-5% as compared to NWC, respectively (Abutaha et al., 2018). The irregular shape and high voids nature of POC affect the propagation of wave through the specimen, is because of the presence of empty voids between and within POC aggregate reduces the pulse velocity through the concrete due to the impeding effect of air (Abutaha et al., 2016). The maximum increment in the UPV value of concrete mixes with the POC powder addition up to 15% had 4.5 km/sec as compared to control mix (POCC) 4.39 km/sec because of reduction in voids as compared to control mix (Nayaka, Alengaram, Jumaat, Yusoff, & Ganasan, 2019).

### 2.5.5 Splitting tensile strength

Tensile strength is the important parameter in plain concrete structures such as dam under earthquake excitations and other structures for example pavement slabs and airfield runways. Which are subjected to tensile strength because these structures are designed based on the bending strength. Therefore, the splitting tensile strength is more significant than compressive strength for designing such types of structures (Yan, Xu, Shen, & Liu, 2013). The tensile strength of concrete is approximately 10% of its compressive strength, concrete is very week in tension (Mohammed et al., 2013). The concrete-based on LWA has lower splitting tensile strength than NWC (Kockal & Ozturan, 2011). The substitution of lightweight aggregate with normal weight aggregate has a symbolic reduction or negative effect on the tensile strength of concrete but may be increased in the compressive strength (Hamada, Jokhio, et al., 2019). The splitting tensile strength of POCC has reduced by increasing the substitution levels of POC with granite because of the porous nature and irregular structure. The at 28 days splitting tensile strength of high strength POCC had 32% lower than NWC at full incorporation of POC with granite (Abutaha et al., 2018). The low splitting tensile strength of POCC has initially started from coarse POC failure since POC is weaker as compared to the aggregate-matrix interface and matrix. The range of splitting tensile strength of concrete containing oil palm boiler clinker at 28 days of curing had 3.05-3.31 MPa (Aslam, Shafigh, Jumaat, & Lachemi, 2016). The previous study based on results that the range of splitting tensile strength for POC concrete had 1.85 to 2.72 N/mm$^2$ which had approximately 68% of the control mix (Mohammed et al., 2014).

### 2.5.6 Flexural strength

The flexural strength of concrete based on LWA has lower than NWAC. The flexural strength of NWC has in the range of 5-6 MPa with 28 days of compressive strength of 34–55 MPa (Aslam, Shafigh, Nomeli, et al., 2017). The flexural strength of POCC has lower than NWC because of the porous nature, irregular shape, and low aggregate crushing strength of POC aggregate as compared to NWA. The flexural strength of POCC had 15% lower than NWC at full incorporation of POC coarse aggregate with granite and the flexural strength of POCC at 28 days had in a range of 3.75-4.42 MPa (Abutaha et al., 2017). Further research said that the improvement in the flexural strength had achieved up to 5%–25% by the POC powder addition as compared to POCC. From the previous research (Abutaha et al., 2018) that the flexural strength of HPOC concrete had 39% lower as compared to NWC at full substitution with POC aggregate but the flexural strength had increased up to 1 to 9% as compared to HPOC concrete by the of POC powder addition. The reduction in the concrete containing POC aggregate is because of low aggregate crushing resistance and induced premature failure in the POCC as compared to NWC when subjected to flexural load. The presence of internal voids within POC aggregates may cause the early propagation of cracks across the specimen due to which the aggregate failed before the failure of the cement paste of the concrete. The POC powder has a great impact on the flexural strength of POC concrete and optimum 28 days flexural strength obtained at 15% POCP had 6.72 MPa as compared to control mix POC concrete of 5.82 MPa (Ahmmad et al., 2017). The flexural strength of POCC50 and POCC100 had 1.5 % and 2.5 % lower than the control mix of 2.02 N/mm$^2$ at 50% and 100 % substitution of POC fine and coarse aggregate with NWA (Nazreen et al., 2018).

## 2.6 Impact resistance of lightweight aggregate concrete

Concrete is characterized as a quasi-brittle failure and the plain concrete without reinforced has lost all the capacity of loading once the failure has developed due to which limits the application of concrete (Yew, Othman, Yew, Yeo, & Mahmud, 2011). Concrete is considered brittle materials because of lower tensile strength and higher rigidity and compressive strength. There are numerous concrete structures which are subjected to impact, vibrating, and seismic load, besides to the static loads during their service life, and just of theses load are more often responsible to reach the structure to the critical or dangerous stage (Shardakov, Shestakov, & Glot, 2018). The chance of the whole structure or a specific member of the structure exposed to the sudden shock and accidental load. Therefore, it is very essential to know about the structure that is subjected to impact load and has also higher impact resistance and impact capacity been required for such kind of members or structure that withstand the impact load or sudden shock. A typical example of an impact-loaded structure or member of structure that is exposed to impact load is hydraulic structures, airport pavements, industrial floors, highway paving, wall panels, and bridge decks (Mohammadhosseini, Tahir, & Sam, 2018). The method used for determining the impact resistance of concrete had classified into four categories and depending on the impacting methodology and parameters (Yoo & Banthia, 2019) such as (a) methods based on kinetic energy; in this method the mass which strikes the specimen very quickly, (b) the method based potential energy; in which a large mass free fall on the specimen, (c) the method in which work done by the hydraulic machine to fracture the test specimen at a medium rate, and (d) method based on the stress wave propagation; in this method, the test specimen has impacted by stress wave propagated through a long steel bar. Some of the tests performed according to the above methods loading condition and test specimens are (a) drop-weight impact test, (b) Charpy impact test, (c) Izod impact test, (d) Gas gun impact test, (e) Fiber pullout impact test, (f) Split Hopkinson pressure bar (SHPB) test, (g) Free falling ball test, (h) Strain energy impact test system, (SEITS), and (i) Projectile impact test. The mostly commonly and simplest test method used for the determination of the impact resistance of concrete has drop-weight method and based on the potential energy mechanism. Many previous studies (Ismail & Hassan, 2019; Mo, Yap, Alengaram, Jumaat, & Bu, 2014; Mohammadhosseini et al., 2018; Omar & Hassan, 2019; Poongodi & Murthi, 2020) that used the drop weight method for the determination of impact resistance of concrete based on LWA.

The coarse aggregate plays an important role in the impact-resistant of concrete because it acts as a barrier to the propagation of crack. The impact resistance of lightweight aggregate concrete based on OPS uncrushed coarse aggregate has higher as compared to OPS crushed coarse aggregate because uncrushed OPS coarse aggregate has a lower impact value than the crushed coarse OPS aggregate and resists the impact load by their orientation and shape of the aggregate during the sudden load (Mo et al., 2014). The impact resistance of lightweight OPS geopolymer concrete (OPSGPC) based on uncrushed OPS coarse aggregate has higher but low compressive strength than OPSGPC with OPS crushed coarse aggregate because of low AIV value of uncrushed OPS coarse aggregate, and resist the sudden load by their orientation, and shape of the aggregates during the impact test (Islam et al., 2017). Further research said that the impact ductility index of concrete based on uncrushed OPS coarse aggregate were than crushed OPS, because of the lower AIV value of uncrushed OPS as compared to the AIV of crushed OPS. Generally, the LWAC has brittle, while the OPS based concrete has ductility characteristics. The concrete specimen with substitution of 40% fine bone china aggregate with normal weight fine aggregate had higher first crack and finial crack impact resistance as compared to control mix (natural sand) (Siddique, Shrivastava, Chaudhary, & Gupta, 2018). From the previous research based on test results (Ismail & Hassan, 2019) that the impact resistance of concrete had significantly reduced with low binder content, high coarse/fine aggregate ratio, and also reduced when exposed to thawing and freezing cycles but no serious effect had observed on the impact resistance with the changeable in the size of coarse aggregates. The reduction in absorbs impact energy by 7% for the coarse aggregate changed from 10 mm to 20 mm.

## 2.7 Acoustic emission method

A vast resource is required for the maintenance, repair, and commissioning of the civil structures in terms of finance, materials, and labor, etc. It is very important for the proper maintenance, monitoring, and repairing of these civil structures to increase the service life of the existing structures, and ensuring the safe operation of the structures subjected to a dynamic or static load. Otherwise, the failure of civil structure causes many economic, and social problems, therefore, it is very important for the appropriate, and well monitoring and capabilities of these structures but it is very difficult to monitor, and look after these structures manually without the application of the instruments. For this purpose, the application of instruments, sensors to monitor these structure integrities, availability of the proper technical method, and knowledge will easily indication of early cracks initiation, fracture, and impending failure.

Concrete is the most important construction material and used for construction purposes worldwide because of its importance. It is very essential to know about the repair, maintenance, and proper monitoring of the cracks, propagation of the cracks, and concrete structure failure. For this purpose, the process for the proper monitoring, damage diagnosis, and the identification of the strategy of the concrete member or structure is known as Structural health monitoring (SHM) closely related to the secured service life of the structure (Świt, 2018). The application of advanced technology for the evaluation of the damage is a great impact on the structural health monitoring part. Therefore, it is very important to evaluate the location, fracture, potential damage, and its impact on the condition of the concrete structure is an important part of service life assessment. For this, it is very essential to know relevant methods that should detect the cracks, deterioration, destructive process, and enable to monitor the progress of damage, and cracks within the entire structure or part of the structure during its routine exposure to various types of operations.

There are many NDT methods for the detection of crack, propagation of cracks, fracture, and failure of the member or entire structure are such as electrochemical methods, electromagnetic (EM) methods, optical sensing methods, and elastic wave methods. While the AE is the advance, unique, non-invasive, passive type of NDT elastic wave method, and good complementary to the UPV, and impact echo (IE), elastic wave methods based on the elastic wave damage detection (Zaki et al., 2015). The application of the AE method is the best choice as compared to other methods based on their results for the identifying of the active destructive process, monitoring, and tracking of their development in various types of structures are such as gas pipeline, Steel Bridge, my Thuan Bridge, and steel column during the routine operation or real-time under different load (Świt, 2018). The damage caused by the various operations such as the mechanical loading, freeze-thaw cycle, restrained shrinkage, and others due to which the cause the damage such as cracks initiating and propagating can be detected and assessed by using the NDT testing AE method for capturing the energy released and signal during the cracking process when crack initiated and propagated (Qian et al., 2014). The application of the acoustic emission gives much information about the rocks damage such as damage mechanism and the properties of the produced cracks such as crack length, direction, etc. due to this information the engineer may be able to know about the behavior of rocks under different loading (Ebrahimian, Ahmadi, Sadri, Li, & Moradian, 2019). The AE method has strong candidates for other NDT methods because it detects and assesses the corrosion in the concrete structure in real-time at the early edges of the onset of corrosion (Zaki et al., 2015). The AE is very sensitive for the detection of growth, initiation of cracks in concrete, and able to identify and detect the corrosion in the concrete at an early stage because of micro-cracks induced in the concrete member or structure when the consequence of the corrosion reaction (Ing, Austin, & Lyons, 2005). The AE method is a very powerful full technique because of its sensitivity to detects processes such as micro-crack formation, growth, movement of dislocation group, fracture, slip or debonding of precipitates (Mazal et al., 2015). The benefits of the AE method are the ability of testing of whole structure without any disturbing for the potential defect's localization.

From the previous research (Nair & Cai, 2010) that explained the basics of AE method is defined as the class of phenomena that works based on the elastic wave that the transit elastic wave is generated by the rapid release of energy from a localized source or sources within a material or the transient elastic wave(s) so generated. Two integral components are an essential requirement for the acoustic emission monitoring system, firstly; the source or the production of an elastic wave that is the deformation materials, secondly; the receiver that receives the stress wave generated from the deformation material or source is known as transducers. Acoustic emissions had classified into two categories as primary emission and secondary emission. The primary emissions are those which are originating from the source of materials interest while secondary emission has been referred to all those emissions originating other than a source of materials. The acoustic emission monitoring strategy had divided into two types according to their adoption either globally and locally. The global AE monitoring is defined as the monitoring of the entire integrity of the structure while the local monitoring strategy is the monitoring of the damaged part of the structure. The principal working of the AE method is shown in Figure 2.1.

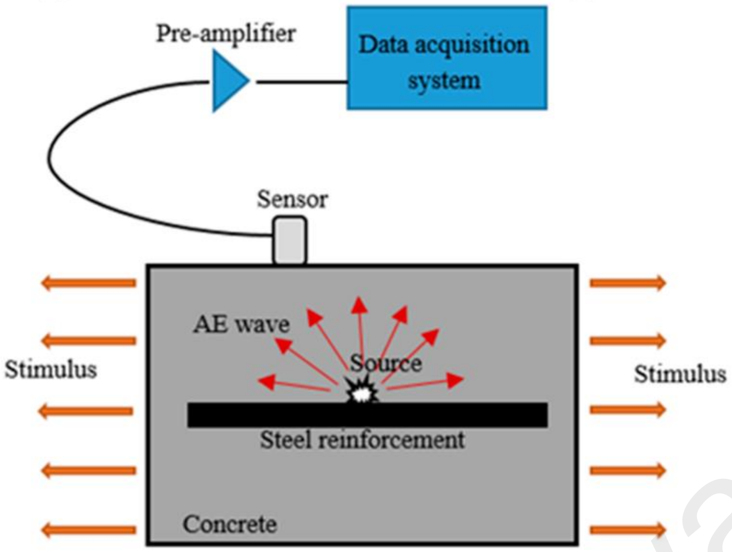


**Figure 2.1: Principal working of acoustic emission method in steel reinforcement concrete (Zaki et al., 2015)**

### 2.7.1 Acoustic emission (AE) parameters

The analysis of damage detection by acoustic emission is classified into two methods for the analysis of the output of AE data are conventional method or also called a parameter-based AE technique and the second method is known as signal-based AE technique or quantitative. The analysis based on signal AE technique is related to the sensor, voltage, resolution, and time (Shahidan et al., 2011) while the analysis based on parameter AE technique has better for the characteristics of the material source by the analysis of AE parameters such as events, signal strength, hits, and energy demonstrate for the detection of damage process such as initiation of crack, crack propagation, deterioration process, and enable to monitor the progress of damage, and cracks within the member or the entire structure (Zaki et al., 2015). The two parameters such as absolute energy and cumulative signal strength were used for the detection of the first crack, growth of the crack, fracture of the specimen, and ultimate crack under a torsional loading in real-time. From the previous research based on the test results analysis and visual inspection of the test specimens (Shahidan, Abdullah, & Ismail, 2016) that the two parameters of AE technique named absolute energy and signal strength are a better indicator for the indication of the real damage mechanism in a concrete structure, and more usable, and effective system for the classification of damage in real-time under loading. The AE parameter absolute energy is defined as the absolute value integral of voltage versus time and this parameter is used for the extent of damage in the concrete material (Shahidan et al., 2016). The signal strength has defined as the measured area of the rectified AE signal with units proportional to volt-seconds, and the AE parameter b-values analysis and cumulative signal strength were found a better tool for the indication of growth of crack as well as identifying the microcracks formation, and macrocracks in RC beam-column joint (Noorsuhada M.N et al., 2017).

### 2.8 Torsional behavior

The torsional load in a structure is defined as the load that twists the elements of the structure around the axial-axis. The torsional behavior of concrete member or structure is highly important as compared to other main forces such as bending, shear, or axial because the torsional loaded member will result in the commencing of the torsion with the combination of compression, tension, flexural, and shear loading or commencing before them because the torsion has highly dependent on the tensile strength of the concrete (George & Sofi, 2017). Torsion form is one of the important and basic structural actions other than compression, tension, bending, and shear loading. The trends of the structures have emerged as irregular and complex structures because of the increase in the diversity of architectural styles, and functional requirements subjected to the earth quick have exposed to the combined loading such as compression, shear, flexural, and torsion. When the incorporation of the torsion stress in the structural member reduced the load-carrying capacity of the structures as compared to the structure or structure member subjected to the combined shear, flexural, and compression loading (Cao, Wu, & Li, 2019). Typical examples of the structural members that are exposed to torsional moments are such as utility poles, spiral staircases, spandrel beams in the frames of buildings, and beams that are curved in plan, as well as earthquake-resistant structures (Rahal, 2013). In such structure members, it is very necessary to consider the torsional characteristics to prevents or avoids torsional damage inside such structures. From the previous study based on results (Yap, Khaw, et al., 2015) that the pre-cracking torsional behavior of concrete based on LWA and NWC such as cracking torque, and initial torsional stiffness had comparable, and equal to 210 $kNm^2$, and 5.5 $kNm^2$, respectively but concrete based on LWA had higher pre-cracking torsional ductility as compared to the NWC because of the 50% higher cracking twist than NWC. The torsional behavior of lightweight concrete based on coconut shell (CS) aggregates had comparable to the conventional concrete, and the concrete specimen with coconut shell had higher resistance to the ultimate torque, and more ductile as compared to the  NWAC because of the natural fibrous structure of CS materials (Gunasekaran, Ramasubramani, Annadurai, & Chandar, 2014). From the previous study based on results (Wang, Liu, & Zhang, 2016) that the recycled aggregate concrete beam under cyclic torsion had 20%, and 7% higher energy dissipation capacity and ductility factor as compared to the conventional concrete beam.

### 2.8.1 Torsional crack

The torsional failure is very dangerous as compared to flexural or shear failure if there is no proper torsional reinforcement. The torsional failure of the torsional-loaded concrete member is more important to investigate as compared to flexural or shear failure because it happens or develops before the commencing of flexural failure (George & Sofi, 2017). From the previous study (Okay & Engin, 2012) based on the experiments that the specimens of unreinforced high strength concrete failed with the formation of the first crack subjected to pure torsion because of the absence of reinforced. Besides other forces such as flexural, shear, and axial; torsion form is one of the basic structural actions. The torsional loading generally occurs with the combination of flexural and shear loading.

When there is no alternative to resist the external load while by the torsion then the structure is exposed to primary torsion (Rao & Seshu, 2006). The torsional failure of a concrete member has originated by the development of the tensile stress because of pure shear state which arises because of torsion (Rao & Seshu, 2003). The crack width of the concrete beam based on the recycled aggregate (RA) under torsion had higher than NWC but the failure process with spiral cracks of the RAC torsion beam had identical to that of the conventional aggregate concrete (Wang et al., 2016). Concrete based on LWA commencing the torsional failure of a concrete member before the flexural or shear failure of the concrete member (Yap, Alengaram, Jumaat, & Khaw, 2015) because of the low tensile strength of LWAC. The significance of evaluating the initial crack and ultimate crack formation has for structural integrity and performance (Shahidan et al., 2016). The detection of cracks in any material or structure is very necessary because of the limitation of location, strict action to repair the cracks, limit the coast related to the rehabilitation work, serviceability, and integrity of the structure.

## 2.9 Research gaps

The research gaps from the fore-mentioned discussion on the literature are summarized in Table 2.3 as shown below.

**Table 2.3: Summary of research gaps in palm oil clinker concrete (POCC)**

<table>
<tr><th>Year</th><th>Authors</th><th>Findings</th><th>Research Gaps</th></tr>
<tr><td>2013</td><td>Mohammed et al.</td><td>The structural behavior and failure mode of the reinforced POCC beam under shear is similar to that of reinforced conventional concrete beam</td><td rowspan="2">-To access and compare the hardened properties of POC concrete at different replacement levels of POC with granite.<br><br>-To investigate the cracking and ultimate torque with their cross-ponding twists of concrete with the different substitution levels of POC with granite.</td></tr>
<tr><td>2016</td><td>Ibrahim & Razak</td><td>The substitution with POC reduced the compressive strength and density of the concrete. However, the coefficient of permeability and porosity rose.</td></tr>
</table>

| **Table 2.3: Summary of research gaps in palm oil clinker concrete (POCC) (cont'd)** | | | |
|---|---|---|---|
| 2016 | Ahmmad et al. | The replacement of OPS by POC as coarse aggregate has a significant positive impact on compressive strength, modulus of elasticity and UPV | -To evaluate the torsional behaviors such as initial torsional stiffness, initial and ultimate torsional toughness.<br><br>-To know the method that detect the cracks, deterioration process, and capable to monitor the progress of damage, and cracks within the entire concrete member in the real-time application of loading.<br><br>-To investigate the localization of torsional cracks in POCC by using the AE parameters such as absolute energy and cumulative signal. |
| 2017 | Abutaha et al. | Curing had a marginal effect on the properties of the concrete rather it is dependent mainly on the properties of the aggregate, and abrasion resistance of the concrete was improved when full water curing was adopted | |
| 2018 | Abutaha et al. | The incorporating additional POCP as filler material by adopting Particle-Packing (PP) method improved the engineering properties of POC concrete | |
| 2019 | Hamada et al. | To use green and sustainable materials that have great benefits to the environment and cost less if compared with the conventional materials. | |

# CHAPTER 3: METHODOLOGY

## 3.1 Methodology flow chart

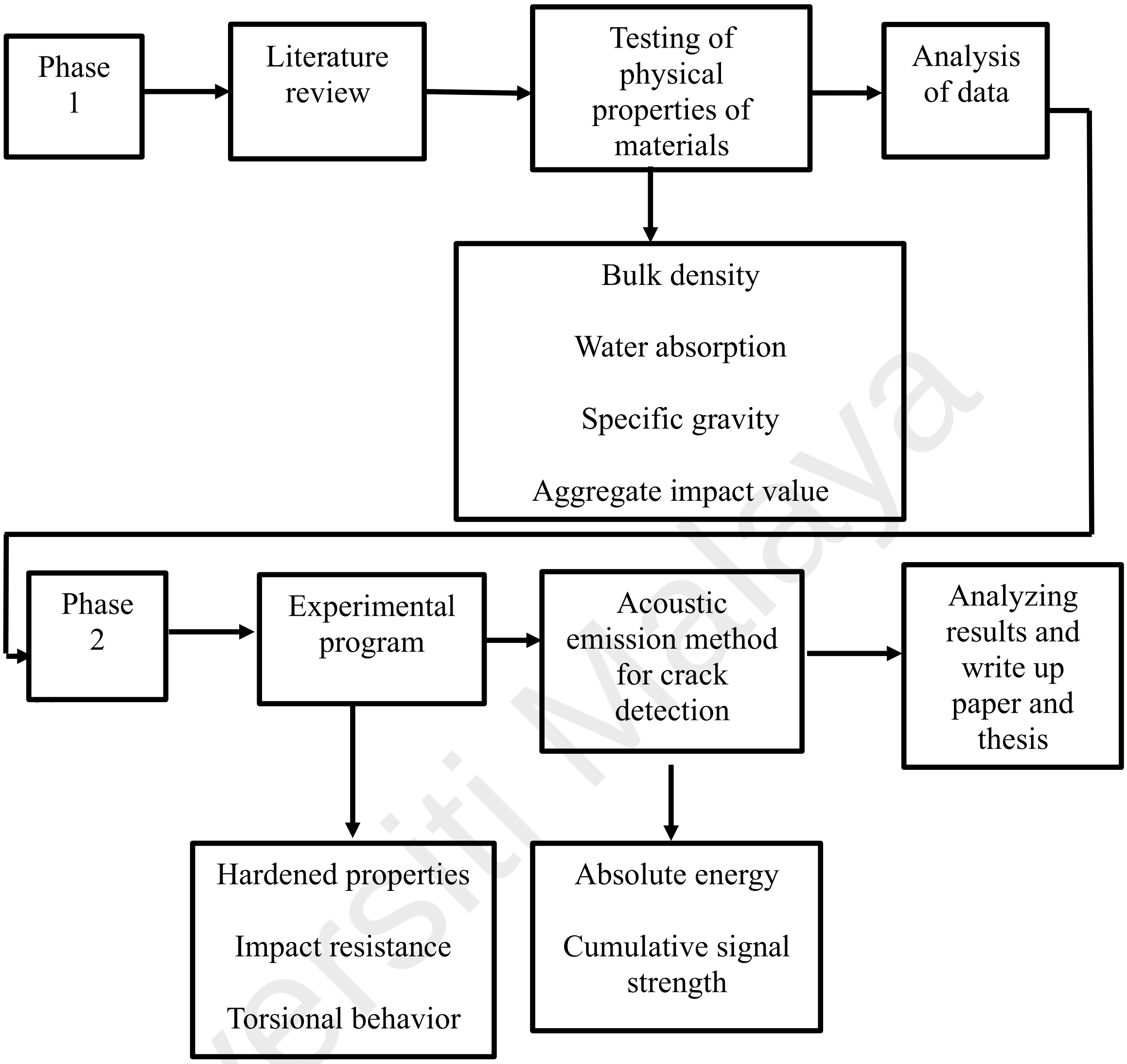


## 3.2 Introduction

In this section of the thesis different materials, methodology, and standards were used for the investigation of the hardened properties, torsional behavior, and torsional crack location of POCC. In addition to the methodology and standards, the physical properties of materials are also explained in this chapter. The contents of this chapter are being entitled to subsections are follows.

## 3.3 Materials used

Various materials were used for the experimental investigation of this research explained in this section, including cement, water, fine aggregates (sand), and coarse aggregates (granite, POC).

### 3.3.1 Cement

Cement used for all mixes in this research was ordinary Portland cement of type 1, 42.5 grade. The Blaine specific surface area and specific gravity were 3510 $cm^2/g$, and 3.14 $g/cm^3$, respectively, and was used in concrete as binder material. The OPC cement used for all the mixes was purchased from the Tasek Corporation Berhad and satisfied all the requirements according to (MS 522: PART 1:2003, 2003) standard. The cement has stored in bags that have water protective with plastic to avoids the cement from moisture.

### 3.3.2 Water

The water used for all the mixes and curing process was potable tap water with a pH value of 6.20. All the concrete specimens that were prepared for all the mixes were kept in the water tank in the laboratory for the specific period of the curing process. All mixes were prepared with a water-cement ratio of 0.5 for this study.

## 3.4 Aggregates

The aggregates used in this study were the fine aggregates and coarse aggregate. The fine aggregates consisted of sand and the coarse aggregates consist of granite and palm oil clinker. The physical properties of sand, granite, and palm oil clinkers such as specific gravity, bulk density, aggregate impact value (AIV) and water absorption, are explained below.

### 3.4.1 Fine aggregate

The fine aggregates used in this research was the river sand for the production of the control mix and POCC. The size of the river sand passes through 4.75 mm and is retained on a 150 µm sieve. The physical properties of river sand are shown in Table 3.1.

**Table 3.1: Physical properties of fine aggregate**

| Properties | River Sand |
|---|---|
| Aggregate size (mm) | <4.75 |
| Specific gravity (SSD) | 2.50 |
| Specific gravity (oven dry) | 2.40 |
| Apparent Specific gravity | 2.64 |
| Water absorption (%) | 4.12 |
| Bulk Density (loose condition), kg/m$^3$ | 1571.50 |
| Bulk Density (compacted condition), kg/m$^3$ | 1706.92 |

### 3.4.2 Coarse aggregates

In this research, crushed granite, and POC were used as coarse aggregate with the size in the range between 4.75-20 mm, and 4.75-14 mm. The crushed granite is locally available from the crushing plant. While the POC aggregate is a byproduct of the palm oil industry and obtained from the industry in the form of a chunk. The chunk form of POC was then crushed with jaw crusher in a laboratory and then sieved to the required sized. Chunk and the coarse forms of POC aggregate are shown in Figure 1.1. To ensure that POC can be suitable to use in the production of concrete it can be tested in terms of specific gravity, bulk density, void ratio, water absorption, and impact value. The physical properties of crushed granite and POC coarse aggregate are seen in Table 3.2.

**Table 3.2: Physical properties of coarse aggregates**

| Properties | Coarse Aggregates | |
|---|---|---|
| | Granite | Palm Oil Clinker (POC) |
| Aggregate size (mm) | 4.75–14 | 4.75–14 |
| Specific gravity (SSD) | 2.60 | 1.54 |
| Specific gravity (oven dry) | 2.59 | 1.40 |
| Apparent Specific gravity | 2.62 | 1.61 |
| Water absorption (%) | 0.40 | 9.38 |
| Aggregate impact value (%) | 20.47 | 47.88 |
| Bulk Density (loose condition), kg/m$^3$ | 1431.71 | 599.99 |
| Bulk Density (compacted condition), kg/m$^3$ | 1572.03 | 694.37 |

### 3.4.3 Bulk density

The bulk density of both fine aggregate (sand) and coarse aggregate (granite and POC) were determined by using the standards-based on (BS EN 1097-3:1998, 1998). Bulk density is of two types; loose bulk density, and compacted bulk density. The procedure followed for the determination of the bulk densities of fine and coarse aggregates is explained as follows.

First of all, the weight and volume of the container were taken as $W_1$ and $V_C$. After this, for loose bulk density, the container was filled loosely with aggregates without any compaction. The over surface aggregates on the container were removed by rod and level the surface. The weight of aggregates with the container was taken as a $W_{L1}$.

For compacted bulk density the container was filled with aggregates in three layers with each layer taper for 25 blows by using the rod. The excess aggregates on the surface were removed, and level the surface, and taken the combined weight of the container with compacted aggregate as a $W_{CL}$.

Both compacted and loose bulk densities are calculated from the following equations 3.1 and 3.2.

$$\text{Bulk density (loose)} = \frac{WL_1 - W_1}{V_c} \tag{3.1}$$

$$\text{Bulk density (compacted)} = \frac{W_{CL} - W_1}{V_c} \tag{3.2}$$

Where,

$V_C$ = Volume of a metallic container

$W_1$ = Weight of metallic container (g)

$WL_1$ = Weight of aggregate (loose) with container (g)

$W_{CL}$ = Weight of aggregate (compacted) with container (g)

### 3.4.4 Specific gravity and water absorption

The Specific gravity and water absorption of fine aggregate (sand) and coarse aggregate (granite and POC) were determined simultaneously. The procedure was carried out for the specific gravity of granite, POC, and sand on the specification based on (ASTM C127 - 15, 2015). The specific gravity is divided into three types, saturated specific gravity, apparent specific gravity, and oven-dry specific gravity.

The water absorption and Specific gravity of sand, granite, and POC coarse aggregate were calculated from the Equations (3.3) - (3.6).

$$\text{Specific gravity (SSD)} = \frac{W_3}{W_3 - (W_1 - W_2)} \tag{3.3}$$

$$\text{Specific gravity (Oven} - \text{dry)} = \frac{W_4}{W_3 - (W_1 - W_2)} \tag{3.4}$$

$$\text{Specific gravity (Apparent)} = \frac{W_4}{W_4 - (W_1 - W_2)} \tag{3.5}$$

$$\text{Water absorption (\%)} = \frac{W_3 - W_4}{W_4} \times 100 \tag{3.6}$$

Where

$W_1$ = Weight of aggregates in water with cylinder

$W_2$ = Weight of water with cylinder

$W_3$ = Weight of SSD aggregates

$W_4$ = Weight of Oven dry aggregates

### 3.4.5 Aggregate impact value

The aggregate impact value (AIV) of POC and granite has been determined according to the standard (BS EN 1097-2:1998, 1998). The AIV of POC and granite is defined as the resistance to the sudden load, shock, or impact. The aggregate impact value of granite and POC is calculated from Equation 3.7.

$$\text{Aggregate impact value} = \frac{M_2}{M_1} \times 100 \tag{3.7}$$

Where

$M_1$ = Mass of the test aggregates (g)

$M_2$ = Mass of the aggregates pass through 2.36 mm test sieve (g)

### 3.5 Preparation of materials

For the preparation of the concrete specimen, firstly the chunk of POC aggregate (Figure 1(a)) was crushed by using the crushing machine, and then getting coarse aggregate (Figure 1(b)) was sieved to pass through 14 mm and retained on 5 mm sieve. After sieving, the POC had soaked in water for 24 hours to fills all the voids of POC coarse aggregate with water to avoid the addition of extra water to the mixing process because POC have higher water absorption than granite. After 24 hours, the POC was kept in an air-dried condition to attained the saturated surface dried (SSD) condition. While the granite and sand were washed to clean off all the clay, dust, fine particles, and then allowed to dried. After that, granite and sand were sieved, and then taken those that passed through 20 mm, and retained on 5mm sieve, and for sand that passed through 5 mm, and retained on 150 µm sieve, respectively.

### 3.6 Mixing proportions

For the mixing proportion, the DOE method was used for the designing of a control mix of grade 40 MPa with a slump value between 60-180 mm. One of the mixes was the control mix with no POC and 100% granite. In the other five mixes, granite was substituted with increasing amounts of POC at replacement levels of 20%, 40%, 60%, 80%, and 100%. For identification, the mixes were named POC0, POC20, POC40, POC60, POC80, and POC100. All other materials used in this research were kept constant at a water/cement ratio of 0.53, cement 410 kg/m$^3$, water 205 kg/m$^3$, and sand 830 kg/m$^3$ of all mixes, respectively. Detail mix proportions are shown in Table 3.3.

**Table 3.3: Mix proportions of POC concrete**

| Mix ID | Replacement Level of POC | Water cement ratio | Mix Proportion ($kg/m^3$) | | | | |
|---|---|---|---|---|---|---|---|
| | | | Water | Ordinary Portland cement, OPC | River sand | Coarse aggregate | |
| | | | | | | Granite | POC coarse aggregate |
| POC0 | 0% | 0.53 | 205 | 410 | 830 | 935 | 0 |
| POC20 | 20% | 0.53 | 205 | 410 | 830 | 748 | 110.76 |
| POC40 | 40% | 0.53 | 205 | 410 | 830 | 561 | 221.52 |
| POC60 | 60% | 0.53 | 205 | 410 | 830 | 374 | 332.29 |
| POC80 | 80% | 0.53 | 205 | 410 | 830 | 187 | 443.05 |
| POC100 | 100% | 0.53 | 205 | 410 | 830 | 0 | 553.81 |

### 3.6.1 Batching

Batching is defining as the quantity measurement process and an important step to ensure the correct proportion of the quantity of material was used for the casting of the concrete. All materials such as granite, POC, sand, and water were weighted by using the weight balance available in a laboratory.

## 3.7 Mixing and casting

Initially, before the material mixing for casting the procedure started from the inspection of the inner surface of the mixer. The inner surface of the mixer was cleaned with water to remove all the material inside and then was wiped with a cloth to make ready for the mixing of the materials.

After the inspection and cleaning process of the mixer was done and the process of the preparation of all the material used for the casting was finished. Firstly, SSD POC, crushed granite, and river sand were dried mixed for 2 minutes in a mixer to obtain a homogenous mass. This was followed with the addition of ordinary Portland cement (OPC) and covered the opening of the mixer with mixer cover to prevent the escaping of fine particles, and cement and mixed for the next 2 minutes. Next, the water is gently added to the dried mixture and allows to mix for the next 2 minutes. After this, the mixer was stopped to rest the mix for 30 seconds, and during this moment to check the consistency of the wet mix by the ball test method. At last, all water was added to the mixture to get the required slump value and homogenous mass concrete for the next 2 more minutes before ready for the casting.

The fresh composite concrete was then put into the wheel barrel to carry to the casting site. The steel moulds were prepared and put on the vibrator table with a thin layer of oil inside the moulds for easy opening, and demolding after the concrete specimen hardened. After this, a thin layer of wet concrete was poured into the large cylinders of dimensions of 150 mm dia. × 300 mm height and vibrated the first layer for 5 seconds to make compaction for the second layer. The second layer was poured to the large cylinders, and also for all other steal moulds for cubes of 100 mm, and 500 mm ×100 mm × 100 mm, and small cylinders of 100 mm dia. × 200 mm height was vibrated for 5 seconds. At last, the concrete layer was poured into all the steel moulds, and was vibrated for 5 seconds to get a level and smooth surface with the surface of steel moulds. After all the process, the moulds were topped with a plastic sheet to avoid the escape of moisture from the wet concrete to the atmosphere, so that to avoid the plastic shrinkage of the concrete.

### 3.7.1 Curing of the specimens

After the 24 fours of the specimens of fresh concrete inside the steel moulds had hardened and de-molded the hardened specimens for the curing purpose. This hardened specimen was placed in a water area for the curing process which contains potable tap water available in the laboratory. All specimens were kept in water tank for the Were 28 days of curing. The curing process for the hardened specimens is essential because to avoid the evaporation of water which is necessary for the hydration process as well as for hardening and also to prevent the shrinkage crack in the immature concrete when exposed to the hot atmosphere. The curing process was performed according to the specification (BS EN 12390-2:2019, 2019).

## 3.8 Testing of the concrete

After the specific age of curing, the hardened concrete specimens were tested for their specific tests. The test procedure and the specification under which the specimens were tested are explained as follows. For every test, three specimens were prepared, and take the averages of the three values.

### 3.8.1 Compression strength

Cubes of 100 $mm^3$ specimens were prepared for the compression test. The compression test procedure was carried under the specification (BS EN 12390-3:2019, 2019). The ELE (Engineering Laboratory Equipment) was used for the compression test with a capacity of 2000 kN. The compression machine and specimens used for the compression test are shown in Figure 3.1. All the specimens for the compression test were tested with a loading pace rate of 2.4 kN/s as stated in the standard.


**Figure 3.1: (a) Compression testing machine (ELE) (b) Specimens for compression test**

### 3.8.2 Water absorption

The water absorption test was conducted on the cube specimens of dimensions 100 $mm^3$. After 28 days of curing, the specimens were oven-dried to a temperature of 105 C for 24 hours to obtain a constant mass. Secondly, the specimens were cooled at room temperature for the next 24 hours and taken the mass of the oven-dried sample as $M_0$. After this, the samples were fully soaked in water for the next 24 hours. At last, the cubes were isolated from the water, and surface dry with a cloth to attained the SSD condition, and taken the weight of SSD specimens as an $M_1$. The water absorption is calculated from Equation 3.8. The specimens and the set up for water absorption are shown in Figure 3.2.

$$\text{Water absorption} = \frac{M_1 - M_2}{M} \times 100 \tag{3.8}$$

Where,

$M_1$ = Mass of the SSD specimen (g)

$M_2$ = Mas of the oven-dried specimen before immersion (g)

### 3.8.3 Splitting tensile strength

The cylinder specimens with dimensions of Ø100 mm ×200 mm height were tested for the splitting tensile strength and the test was done according to the specification (BS EN 12390-6:2009, 2010). The cylinder was held between the two packing strips placed on the steel holder with its horizontal axis perpendicular to the steel holder and then the steel bar was placed on the cylinder. After this, the steel holder was placed in the compression machine for the test and then applied the load on the cylinder with a pacing rate of 1.767 kN/s.

### 3.8.4 Flexural strength

The flexural strength was done according to the specification (BS EN 12390-5:2019, 2019). The specimens used for the test was the prisms of 500 mm × 100 mm × 100 mm dimensions. The specimens were tested with a pacing rate of 0.067 kN/s using the flexural testing machine EL 33-6090. The flexural machine and specimen used for the flexural test are seen in Figure 3.2.

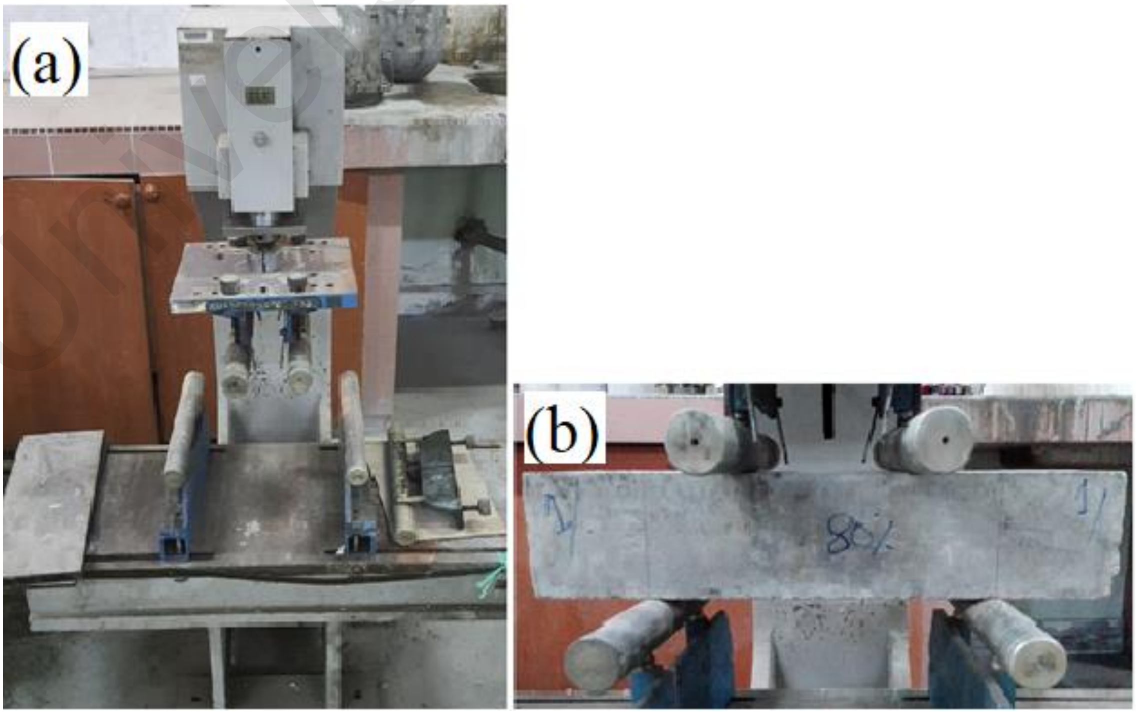


**Figure 3.2: (a) Flexural machine (b) prism for flexural test**

### 3.8.5 Impact test and impact ductility index

The compression cylinder of 63.5 mm dia. × 152 mm length was conducted for the impact test. The procedure followed for the impact test was performed according to the drop-weight test. According to the drop-weight test, the compression cylinder was exposed to the repeated blows on the same spot by using the drop hammer impact machine with a 4.45 kg drop hammer released with a height of 445 mm (ACI, 2002). The steel ball was placed on the compression cylinder placed inside the moulds of the impact machine. The pressure was applied by drop hammer on steel ball repeatedly for the visible first crack and failure crack in the specimen. The number of blows that caused the first and failure cracks were observed and used to calculate the impact energies of the concrete at first and failure crack. The impact ductility index of the concrete is defined as the ratio between the final and initial impact energies. The impact energies at first and failure, and impact ductility index of the concrete are calculated from the given Equations 3.9, 3.10, and 3.11 (Mo et al., 2014). The machine, mould, and specimen used for the impact test are shown in Figure 3.3.

$$\mathrm{E_1} = \mathrm{mgh} \times \mathrm{N_1} \tag{3.9}$$

$$\mathrm{E_2} = \mathrm{mgh} \times \mathrm{N_2} \tag{3.10}$$

$$\mu_i = \mathrm{Nf/Nc} \tag{3.11}$$

Where,

$E_1$ = Impact energy to cause a first visible crack in Joule (J)

$E_2$ = Impact energy to cause ultimate failure crack in Joule (J)

m = Mass of drop hammer = 4.45 kg

g = 9.81 m/s$^2$

h = Releasing height of drop hammer = 445 mm

N = Number of blows

$\mu_i$ = Impact ductility index

Ni = Number of blows to cause first crack

Nf = Number of blows to cause failure


**Figure 3.3: (a) Impact machine (b) Mould and specimen for impact test**

### 3.8.6 Torsion test

Prisms with dimensions of 500 × 100 × 100 $mm^3$ were prepared for torsion test using the torsion machine and their set up is shown in Figure 3.4, and the acoustic emission method to detect the first, and ultimate crack of the concrete. The load was applied by the automated torsion at a constant rate of 0.15 degrees/min on all prisms until the ultimate crack had produced. The crack which is produced at the maximum torsional load is known as the ultimate crack. The torsion-curve was directly measured from the torsion machine and the torque-twist curve was analyzed from the torsion curve. The initial stiffness was calculated as the linear gradient before the first crack commencing while initial and ultimate toughness was calculated as the total area under the initial and ultimate torque-twist curve (Figure 3.5): Part 1 measures the pre-cracking torsional toughness before the first crack formation and Part 2 denotes the cracked torsional toughness before the specimens achieve ultimate torque.

In the acoustic emission (AE) method, four sensors were fixed at two side surfaces on each specimen at a distance of 230 mm between the two sensors shown in Figure 3.4 (a). The sensors were placed in both x and y axis (perpendicular to each other), near the end of both ends, in order to capture the formation of torsional cracks in both x and y axis. The AE method is very sensitive to detects the noise, sounds of the machine, and surroundings, therefore filters had applied up to 40 dB for the purpose to not affect the results. The following checking's were carried out before the performance of the torsion test. Firstly, the AE sensors sensitivity test was performed on the concrete specimen to ensure the well-functioning of all four sensors on the concrete specimens. Secondly, the AE velocity test was performed to measures the AE wave through the concrete, which is very important for the location of AE signals.

The data getting from the Acoustic Emission software (AE win) were analyzed to obtain the absolute energy-twist and CSS-twist graphs. The torque-twist curve from the torsion machine was compared with absolute energy-twist, and CSS-twist curves to analyze the initial and ultimate crack, respectively. The important parameters that analyze were initial crack, ultimate crack, initial torsional torque, and ultimate torque with corresponding twists from the torque-twist of torsion machine with the collaboration of analyzed AE graphs (absolute energy and CSS).

The crack resistance, location of cracks, and pattern of cracks of the specimens at different substitution levels of POC coarse aggregate were investigated by comparing the visual inspection of cracks of concrete specimens with the analyzing data of the location of a crack from the crack mapping and crack profile from AE method.

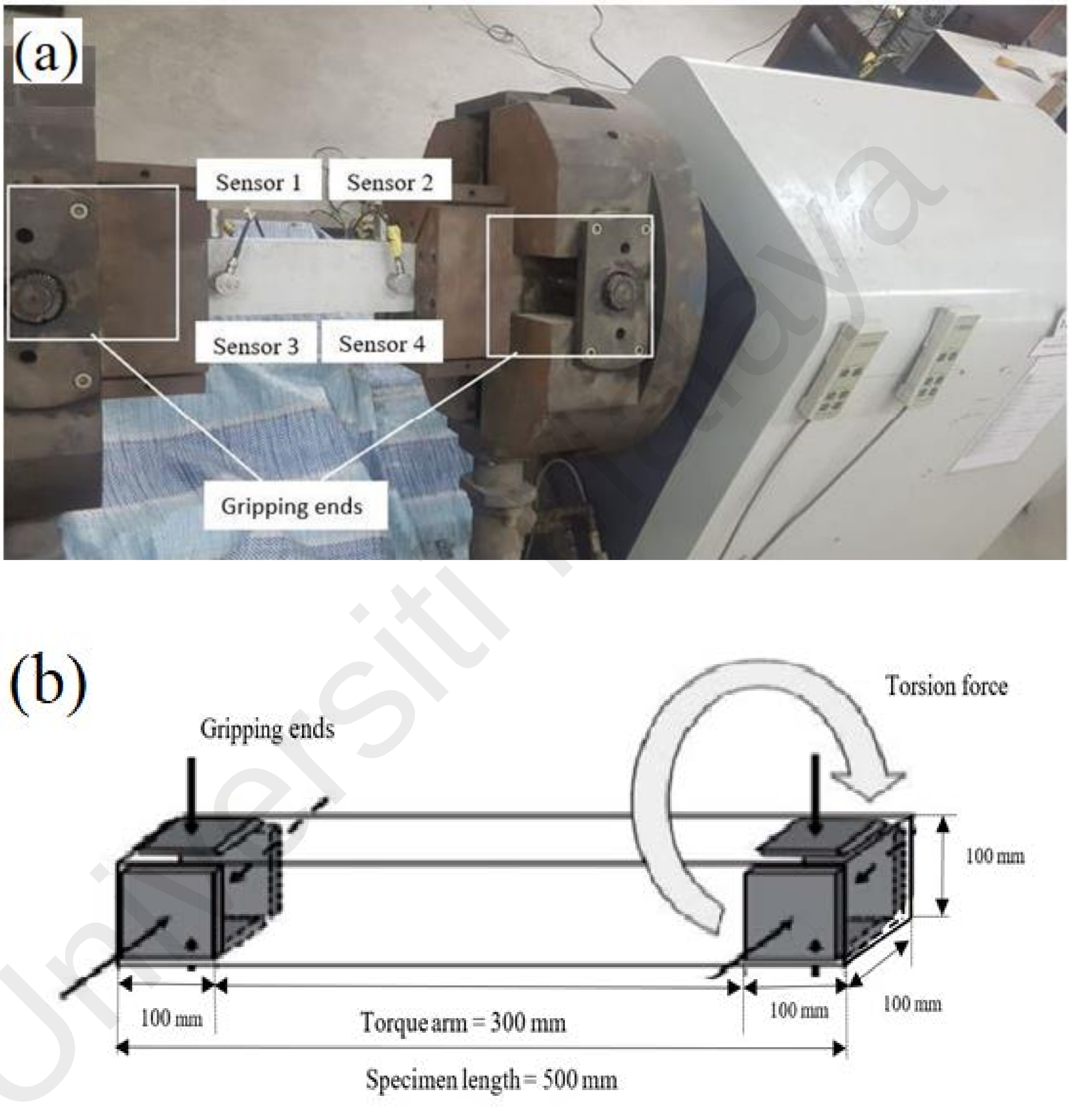


**Figure 3.4**: **(a) Torsion machine and AE setup (b) illustration for torsion test set up**

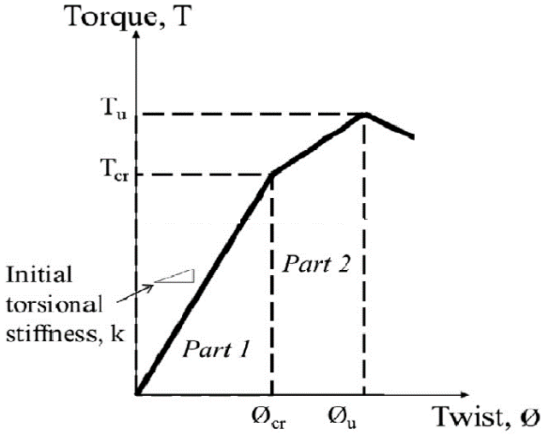


**Figure 3.5: Simplified torsion model (Yap, Khaw, et al., 2015)**

# CHAPTER 4: RESULTS AND DISCUSSION

## 4.1 General

In this chapter, the results obtained from the various tests such as bulk density, specific gravity, water absorption, and AIV for the materials used for the POCC production and the hardened properties, torsional behavior, and crack localization of POC concrete are analyzed and discussed. The variable in this study is the POC at different substitution levels of granite. Six mixes were prepared and analyzed at different replacement levels of POC coarse aggregate will be explained and discussed in this section of the thesis in detail.

## 4.2 Material properties of aggregates

The analysis and explanation of the results of the material obtained from the various tests are discussing in this section of the chapter. The mechanical properties and torsional behavior of POCC are mainly affected because of the properties of the material. Therefore, it is very essential to analyzing and determination of the material properties of aggregates.

### 4.2.1 Bulk density

The bulk density of POC aggregate has almost lower than granite because of the void's nature of the POC coarse aggregate from Figure 1.1. The loose and compacted bulk densities of POC had 599.991 Kg/m$^3$, and 694.37 Kg/m$^3$ while 1431.71Kg/m$^3$, and 1572.03 kg/m$^3$ for the granite, respectively are shown in Table 4.1. From the obtained results that both compacted, and loose bulk densities of POC had 41.90 %, and 44.17 % lower than granite, which is due to higher inner and surface voids of POC (Mohammed et al., 2014; Mohammed et al., 2013). From the previous study, the POC had almost 48% lower bulk density as compared to granite (Mohammed et al., 2014). The difference in the bulk densities of POC and granite was because of the porous nature of POC as compared to granite.

**Table 4.1: Physical properties of granite, and POC**

| Properties | Unit | Granite | POC |
|---|---|---|---|
| Aggregate size | mm | 4.75–14 | 4.75–14 |
| Bulk density (loose condition) | $kg/m^3$ | 1431.71 | 599.99 |
| Bulk density (compacted condition) | $kg/m^3$ | 1572.03 | 694.37 |
| Specific gravity (SSD) | - | 2.60 | 1.54 |
| Specific gravity (oven-dry) | - | 2.59 | 1.40 |
| Apparent Specific gravity | - | 2.62 | 1.61 |
| Water absorption (24 hours) | % | 0.40 | 9.38 |
| Aggregate impact value, AIV | % | 20.47 | 47.88 |

### 4.2.2 Specific gravity

The mass of the aggregate in air dived by the mass of an equal volume of water is known as specific gravity according to ACI E 701.

The specific gravity of POC was lower as compared to granite is shown in Table 4.1. The value of specific gravity in oven-dried condition and SSD condition of POC had 1.4 and 1.54 while 2.59 and 2.6 for granite, respectively.

### 4.2.3 Water absorption

The water absorption of materials has highly dependent on the porous structure of the aggregates. The higher the voids of the materials will be the higher the water absorption. Therefore, the water absorption of POC was higher than the granite because of the porous structure of the POC is shown in Figure 1.1. From Table 4.1 the water absorption of POC was 9.38% which is 23.475 times higher than granite while 0.4% for the granite. The water absorption is also helped out to one to the difference between the mass of the material due to the absorbed of water in the voids within the constituent particles as compared to the dried condition.

### 4.2.4 Impact resistance of aggregates

The aggregate impact test was done to determine the toughness and resistance of the POC coarse aggregate to sudden shock or impact as compared to the granite. It is depicted from Table 4.1; that the aggregate impact value (AIV) of POC was higher as compared to granite which means that the resistance to the impact or sudden shock had lower to the granite. The AIV value of POC was 47.88% which is 2.34 times higher than the AIV of granite of 20.47%.

## 4.3 Mechanical properties of concrete

In this section of the chapter, the analysis and discussing the hardened properties of concrete such as hardened density, compression strength, UPV value, splitting tensile strength, water absorption, flexural strength, and impact resistance at different substitution levels of POC with granite.

### 4.3.1 Hardened density

From the results, the hardened density of the concrete was decreased by increasing the replacement level of POC with granite. The effects of different substitution levels of POC on the hardened density are seen in Figure 4.1. The density of concrete reduced due to the void's nature of POC subsequently reduces the strength of concrete. The maximum reduction in hardened density has occurred at 100% substitution of POC of 1958.68 $kg/m^3$. At the full substitution level of POC, the hardened density of concrete was less than 2000 $kg/m^3$ and 18.84% lower than the control mix of 2413.2 $kg/m^3$. The reduction range of hardened density was between 2.19-18.84% with the 20-100% substitution level of POC with granite. The lower hardened density of POCC was attributed to the lower bulk density of POC 599.99 kg/m$^3$ as compared to granite 1431.708 kg/m$^3$ which is 41.90% less than the bulk density of granite (Table 4.1). From the earlier study (Abutaha et al., 2016) that the POC concrete had 14% lower hardened density at the full substitution of POC was because of the 43% lower bulk density than the normal-weight aggregate.

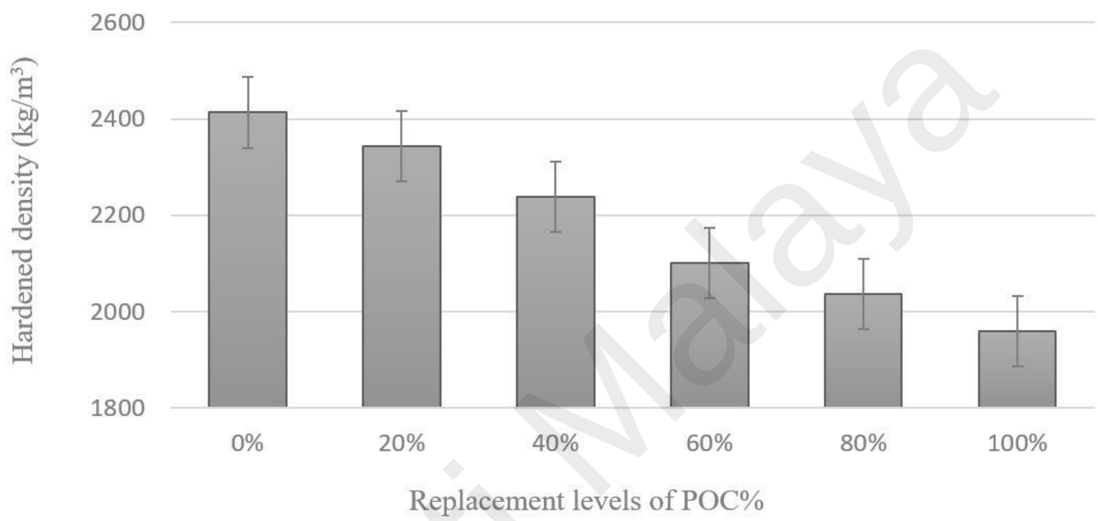


**Figure 4.1: Effect of different replacement levels of POC coarse aggregate on the hardened density**

### 4.3.2 Compression strength

The 28 days of compressive strength of POC concrete is seen in Figure 4.2. The strength of concrete has dependent on the properties of aggregate used are hardened cement paste, and interfacial bonding (Aslam, Shafigh, & Jumaat, 2017). The compressive strength of POC concrete has been decreased due to the high water absorption and porosity of POC aggregates (Hamada, Jokhio, et al., 2019). The compressive strength of the concrete was reduced by increasing the POC. The maximum reduction in the compressive strength of POCC has occurred at 100% substitution of POC of 28.79 MPa. The strength reduction of concrete at 20%, 40%, 60%, and 80% replacement of POC was 21.03%, 24.01%, 30.34 and 32.01% as compared to POC0 mix of strength 45.88 MPa. The decrease in the strength was because of the porous surface and internal voids of POC due to this the load-bearing capacity of POC aggregates reduced to effects the strength of POC concrete. The compressive strength of concrete mainly depends on the aggregates. Aggregates play as the skeleton of concrete, and this means that the strength of aggregates directly affecting the compressive strength. The compressive strength of concrete has shown an inverse relationship with the substitution of POC, because of the higher AIV value of POC as compared to the granite. The strength of POC is lower by having higher AIV (47.88%) as compared to AIV of granite (20.47%) which is 2.34 times higher than the AIV of granite. The high strength of the concrete at 0% replacement of POC is due to a good packing structure, and higher impact resistance as compared to other mixes. The reason is that the irregular shape and less interlocking effect of the POC decrease the packing of the concrete (Kanadasan & Razak, 2015).

The compressive strength of concrete is highly dependent on the hard density of the concrete and the hardened density is one of the most variables to be considered in concrete structure design (Aslam, Shafigh, & Jumaat, 2016). The concrete containing POC has low compression strength and hard density as compared to NWC (Hamada, Jokhio, et al., 2019). The relationship between compressive strength and hard density is shown in Figure 4.3, illustrates that both compression strength and hard density was higher for the control mix, and reduced for the mixes when the incorporation of the POC was increased. The maximum reduction in the compression strength and hardened density was occurred at full substitution of POC of 18.83% and 37.25%, respectively as compared to POC0 mix. The reason is that the difference between the physical properties of POC and granite such as bulk density, water absorption, porous structure, and aggregate impact value are shown in Table 4.1.

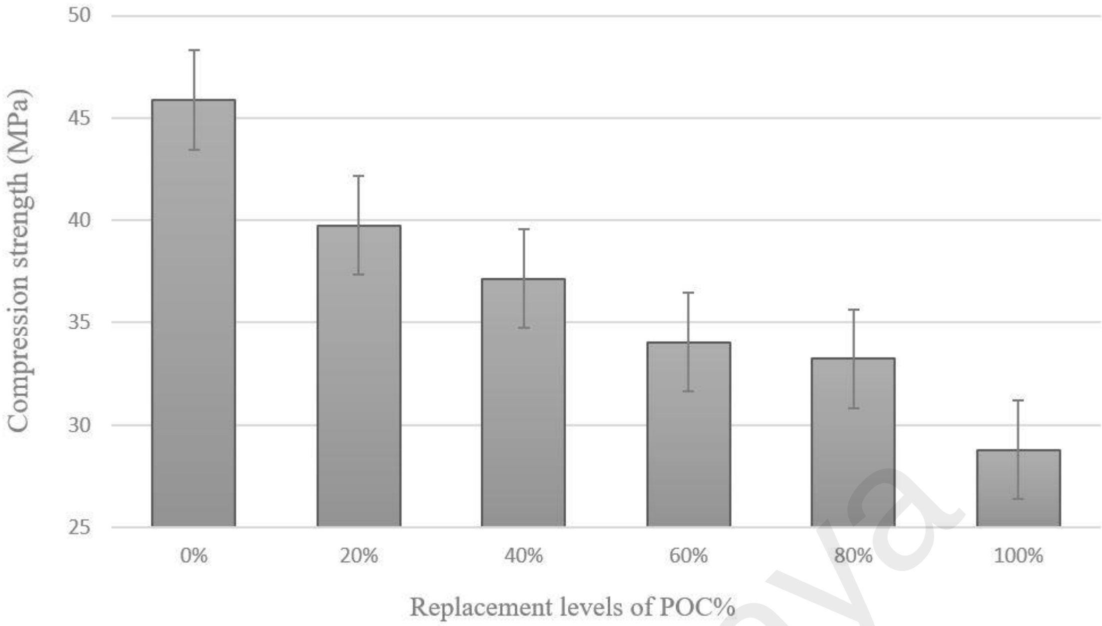


**Figure 4.2: Effect of different replacement levels of POC on the compressive strength**

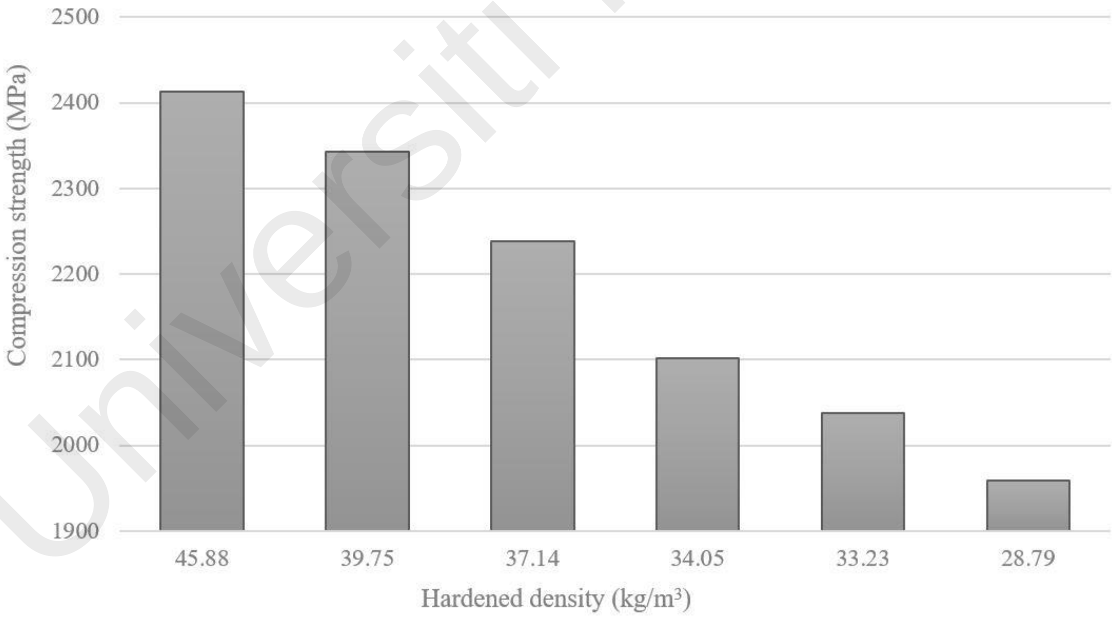


**Figure 4.3: Relationship between compressive strength and hardened density**

### 4.3.3 Ultrasonic pulse velocity

The ultrasonic pulse velocity (UPV) test was performed to determine the consistency, dense, and quality of the concrete to evaluate the occurrence of the cracks, pores, voids, and depth of the cracks. UPV is a non-destructive test that has been performed on the same specimens used for hardened density and compression strength. The UPV values at various substitution proportions are shown in Figure 4.4**.** The UPV values were reduced on increasing the substitution levels of POC in the concrete. The reduction in the UPV value by increasing the POC was because of the occurrence of internal and surface pores, and high-water absorption of POC (Table 4.1). The empty pores between or inside the aggregates decrease the velocity of the pulse through the concrete specimen due to the impeding effect of air (Abutaha et al., 2016; Hamada, Yahaya, et al., 2019) and therefore lower UPV value of POCC as compared to the control mix. From the previous study based on experimental results (Abutaha et al., 2018) that the UPV values in the range of 3.5-4 km/sec and above 4 km/sec fall in a good and very good zone, respectively. The concrete in this range is considered small pores and cracks. All the mixes in this research have possessed the UPV values in the range of 4-5 km/sec and fall in a very good zone which means that all the mixes have very small internal and surface pores due to this faster pulse are transfer through the concrete specimen. The UPV value of the concrete at the full substitution of POC was reduced to 4.09 km/sec as compared to the POC0 mix of 5.09 km/sec. The UPV value at 100% replacement of POC was 80.35 % of the UPV value of the POC0 mix, and reduction can be caused at full substitution of POC was because of the increase in the air content in the concrete with the increase in the amount of POC.

The relationship between hardened density, compression strength, and UPV value of concrete at different substitution levels of POC is seen in Figure 4.5. It illustrated that the compression strength, hardened density, and UPV value of concrete decreased on increasing the amount of POC were because of the physical properties of POC. The maximum reduction in the compression strength, UPV value, and hard density of concrete at the full substitution of POC were 37.25%,19.64%, and 18.83% as compared to the POC0 mix. The reduction in the above properties is due to the irregular shape, lower bulk density, higher impact values, water absorption, internal and external voids of POC as compared to granite.

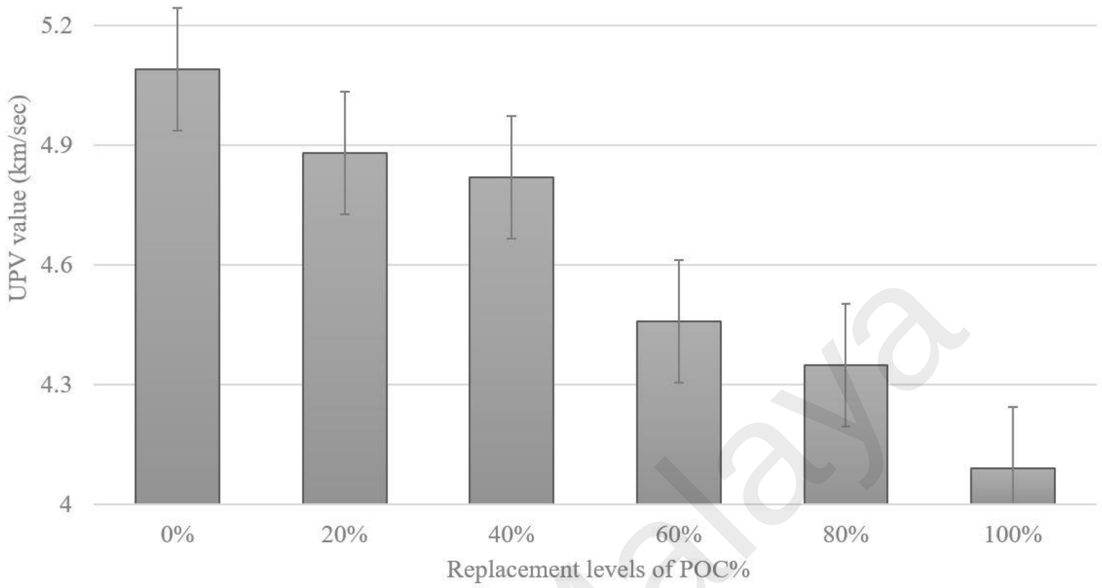


**Figure 4.4: UPV value at different replacement level of POC**

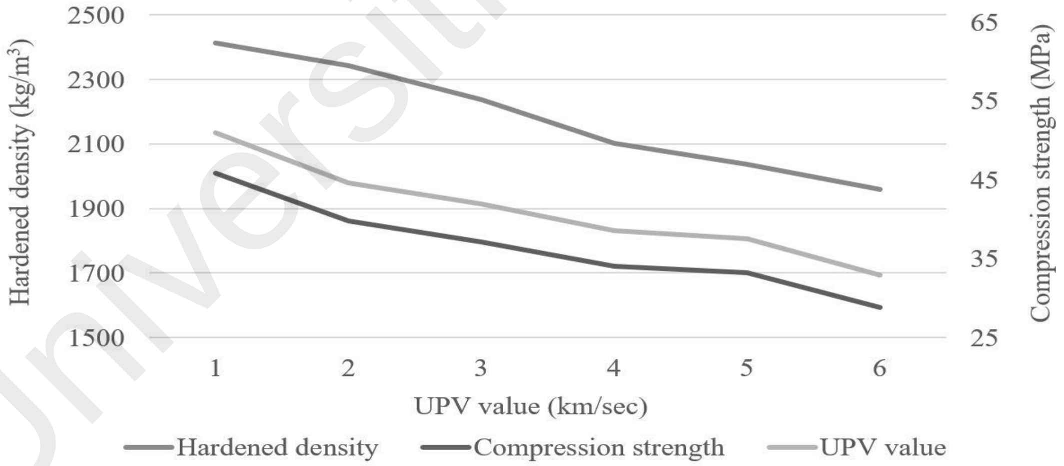


**Figure 4.5: Comparison between hard density, compression strength, and UPV value.**

### 4.3.4 Water absorption

Water absorption is an important factor that affects the durability of concrete and highly dependent on the porosity of the aggregates. Typically the concrete using LWA has higher water absorption than the NWA due to the high range of internal and external pores associated with lightweight aggregate (LWA) (Ahmmad et al., 2017; Topçu & Uygunoğlu, 2010). The water absorption at different replacement levels of POC with granite is shown in Figure 4.6. It is obvious that the water absorption of the concrete was increased by increasing the volume of POC. The water absorption of the control mix was 56.20% lower than at the full substitution of POC. The difference in the water absorption of concrete at different substitution levels of POC was due to the difference in the water absorption of POC and granite clearly shown in Table 4.1. The increase in the water absorption of the concrete with the substitution of POC was due to the higher voids of POC as compared to granite.

The water absorption of concrete is highly dependent on the voids of the coarse aggregates. From the physical properties shown in Table 4.1, that the POC had a higher percentage of voids and water absorption as compared to granite due to this reduction in the UPV value but increase in the water absorption of POCC. The impeding effect of air inside or between the empty voids of POC had increased in the capacity of POC to absorb a large amount of water as compared to granite. The maximum increment in the water absorption of 1.78 times higher at the full substitution of POC as compared to the POC0 mix.

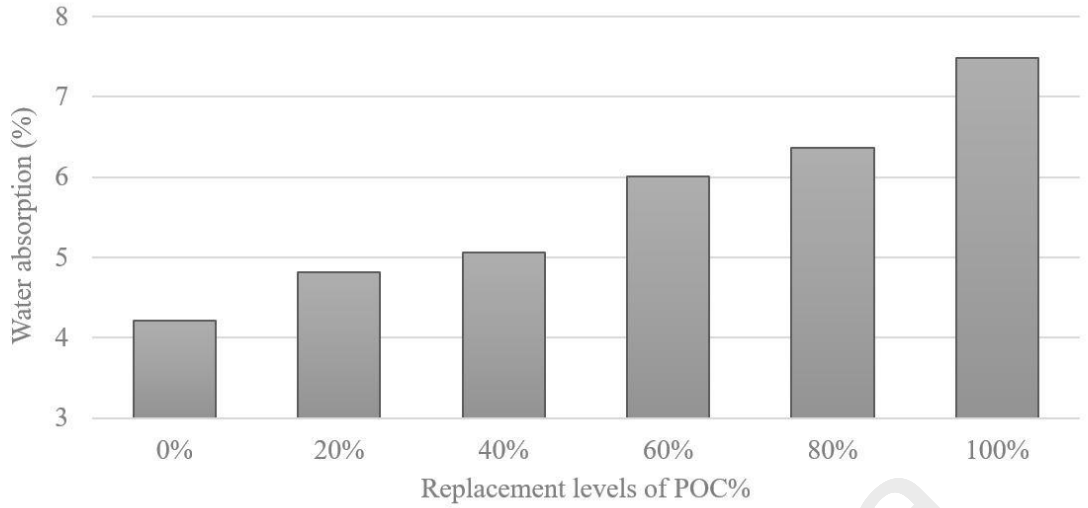


**Figure 4.6: Water absorption at different substitution level of POC**

### 4.3.5 Splitting tensile strength

Referring to Figure 4.7, the splitting tensile strength results show a similar pattern as the compressive strength results. The splitting tensile strength of concrete based on lightweight aggregate has generally lower as compared to NWAC of the equivalent grade of concrete (Haque, Al-Khaiat, & Kayali, 2004). The splitting tensile strength of the concrete was reduced by increasing the replacement levels of the POC are seen in Figure 4.7. The range of splitting tensile strength was between 2.5-3.62 MPa. A maximum reduction in the splitting tensile strength of 30.94% has occurred at the full substitution of POC. The reduction in the strength was due to the failure of the POC aggregate instead of matrix and the aggregate-matrix interface is from the visual inspection in Figure 4.8. Figure 4.8(a) illustrates that the POC0 mix had failed due to the matrix and the aggregate-matrix interface failure while POC100 shows aggregate failure as shown in Figure 4.8(b). The 28 days splitting tensile strength of POC concrete had 16-32% less as compared to NWC (Ahmad, Hilton, Mohd, & Mohd Noor, 2007). The results and observations on splitting tensile strength were comparable to the paper from Abutaha et al. (2018), the splitting tensile strength of high strength palm oil clinker concrete was in the ranges between 3.5–4.8 MPa and given the maximum reduction of 32% at full replacement level of POC aggregate (Abutaha et al., 2018) and the reduction was due to failure of the POC instead of the matrix, and aggregate-matrix interface.

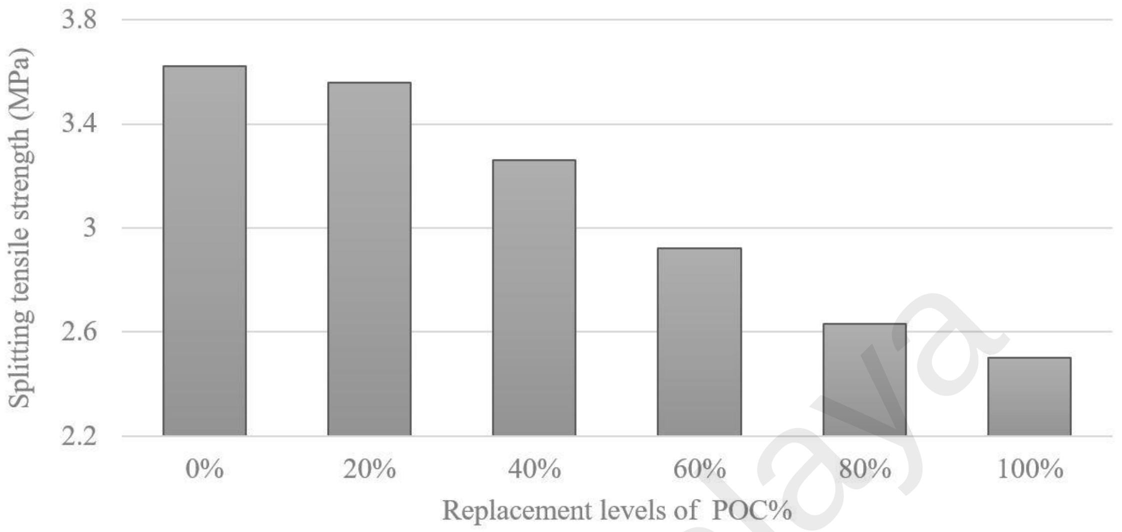


**Figure 4.7: Effect of POC on the splitting tensile strength**

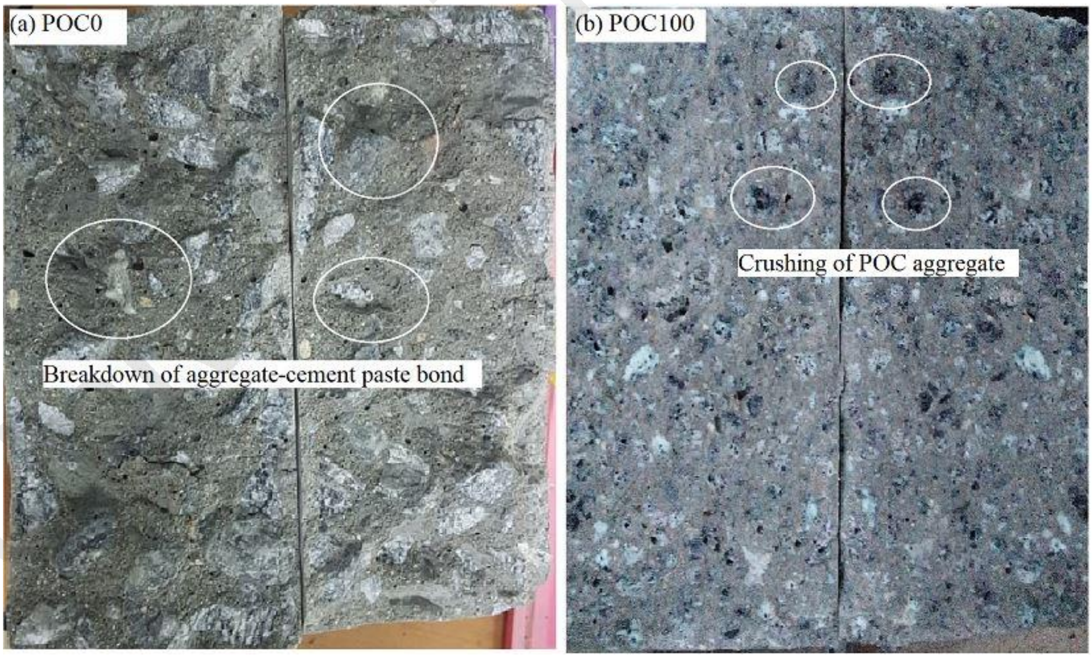


**Figure 4.8: Cross-sections of the failed specimens under splitting tensile test (a) POC0, and (b) POC100 mixes.**

### 4.3.6 Flexural strength

The flexural strength of concrete was decreased by increasing the amount of POC, are seen in Figure 4.9. The maximum reduction in the flexural strength of 14.31% has occurred at 100% replacement of POC. The reduction in flexural strength is due to the low aggregate impact resistance of the POC as compared to granite, and flexural load induces premature failure of POC. The decrease in flexural strength was because of the substitution of POC is due to the failure of POC under the flexural load because of the higher aggregate impact value of POC as shown in Table 4.1. The early crack propagation occurs across the concrete specimens containing POC was because of the internal voids within the POC aggregates, and this will allow the aggregates to fail before the cement paste (Abutaha et al., 2018). The flexural strength of NWC has been reported to be in the range of 5–6 MPa at 28 days with compressive strength in the range of 34–55 MPa (Aslam, Shafigh, Nomeli, et al., 2017). In this work, the flexural strength of all mixes except POC100 was found to be higher than 5 MPa, well within the range found in normal-weight concrete because all the mixes have hardened densities higher than the 2000 kg/m$^3$ except the POC100 mix (Figure 4.1).

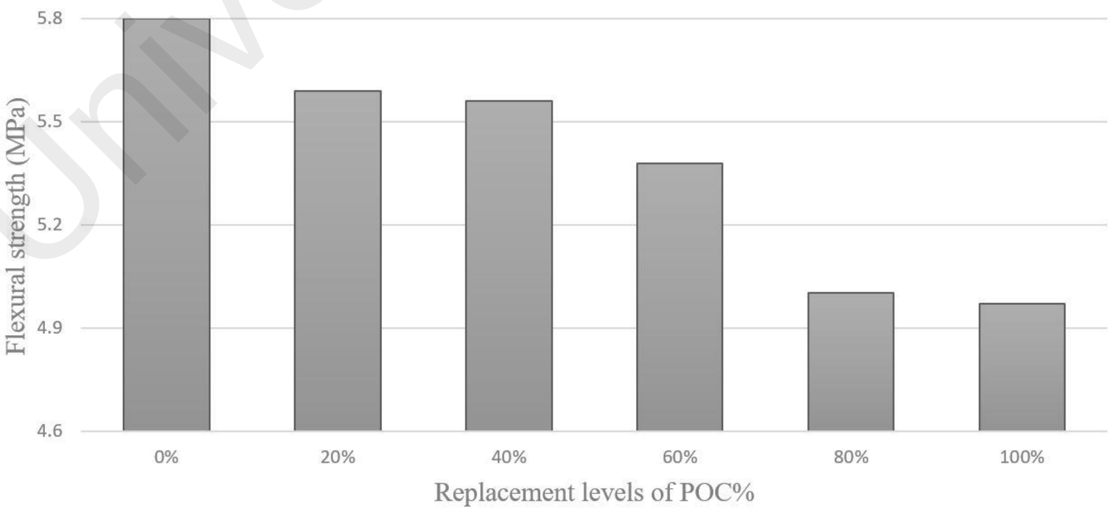


**Figure 4.9: Flexural strength of POC concrete**

## 4.4 Impact resistance

### 4.4.1 First and failure crack energy

The effect of POC coarse aggregate on the impact energy at first and failure cracks of concrete at different substitution levels are depicted in Table 4.2. The impact energy at first and failure crack in this study were almost the same at all different replacement levels of POC. The impact energies were increased up to 60% of the incoperation of POC, and then decreased. The impact energy and the number of blows of concrete at 100% substitution of POC were higher as compared to the POC0 mix. The maximum impact energy at first and failure cracks were given at 60% substitution of POC which was 2274 joule and 2314 joules, respectively, while the impact energies (first and failure cracks) at 60% and 100% incorporation of POC were approximately 4 and 1.60 times higher than control mix. The impact energies and number of blows of POC40 mix were higher in all all mixes except of the POC 60 mix. The coarse aggregate has played a key role in the impact resistance of concrete to reduce the crack propagation, and penetration depth (Zhang, Shim, Lu, & Chew, 2005).

The maximum impact ductility index of concrete was at the 0% replacement level of POC which is 1.07. The higher impact ductility index at 0% substitution level of POC was because of the higher impact resistance, and higher ductility of the granite as compared to the POC. While the impact ductility index of the POC100 mix was similar to the impact ductility index of the POC20 mix of 1.04, which is 2.80% lower than the POC0 mix. Still, the POC based concrete has a comparable ductility index to the POC0 mix, and all impact ductility index is shown in Table 4.2. The impact ductility index of POC40 has lowest in all mixes and similliar to the POC 60 mix which is 1.67%, and 1.2% lower than than POC0, and POC100. The impact and crushing values of POC coarse aggregate have approximately 34% and 30% higher than granite because of the porous, and angular shape of the POC coarse aggregate (Mohammed et al., 2014).

**Table 4.2: Impact test results at different replacement levels of POC coarse aggregate.**

| Mix ID | Blow number to cause the first crack | Impact energy (first crack), Impact,1st, cr (J) | Blow number to cause specimen failure | Impact energy (specimen failure), Impact, fail (J) | Impact ductility index, $\mu_i$ |
|---|---|---|---|---|---|
| POC0 | 28 | 559 | 30 | 598 | 1.07 |
| POC20 | 69 | 1376 | 72 | 1436 | 1.04 |
| POC40 | 102 | 2035 | 104 | 2075 | 1.02 |
| POC60 | 114 | 2274 | 116 | 2314 | 1.02 |
| POC80 | 65 | 1297 | 68 | 1357 | 1.05 |
| POC100 | 45 | 898 | 47 | 938 | 1.04 |

## 4.5 Torsional behavior

Important parameters such as cracking torque, ultimate torque, initial torsional stiffness, initial torsional toughness, ultimate torsional toughness, initial and ultimate cracks were analyzed. The cracking torque and their corresponding twists are the torque and twist at which the first crack formed, respectively. Torsional behavior of concrete at different substitution levels of POC is shown in Table 4.3. The cracking torque of concrete decreased on increasing the substitution levels of POC. The maximum cracking torque occurred at 40% substitution of POC of 54.77 Nm, which is 4.68% lower than the control mix, and 1.3 times higher than the POC100 mix. The POC40 had also higher cracking torsional stiffness of 11.47 kNm$^2$ in all mixes, except the POC0 due to sustained higher cracking torque, at the smallest angle of twist. The maximum reduction in the cracking torque and torsional stiffness (28.42%, and 38.97% lower than cracking torque, and initial torsional stiffness of POC0 of 57.46 Nm, and 12.47 kNm$^2$, respectively), occurred at full incorporation of POC. However, the POC60 sustained cracking torque at the maximum twist of 0.0060 rad/m. The cracking torsional stiffness of concrete is dependent on their tensile strength because a torsional failure of the concrete member is originated by the development of tensile stress is because of the state of pure shear, which begins due to torsion (Yap et al., 2016). Therefore, the POC0 mix had higher tensile strength and higher initial torsional stiffness than all other mixes. However, the initial torsional toughness of all the mixes decreased on increasing the substitution levels of POC. The maximum reduction in the initial torsional toughness occurred at the full substitution of POC– the torsional toughness of the POC100 was 31% lower than POC0 of 0.16 Nm/m – but the twist of POC100 that resisted the cracking torque was almost 8% lower as compared to POC0 mix. The cracking torsional stiffness of all concrete (reinforced or plain) had a linear slope up to the cracking torque because, until the first crack, the torsional stiffness is not dependent on the type of reinforcement of the concrete (Okay & Engin, 2012). Therefore, all mixes showed a linear torque-twist response up to the first crack or cracking torque from the torque-twist graph as seen in Figure 4.10.

The torsional capacity of concrete depended on the concrete strength, but the cracks at which concrete failed were more sudden and brittle, because of the absence of reinforcement or plain concrete (Okay & Engin, 2012). The ultimate torque decreased on increasing the replacement levels of POC (Table 4.3). The POC40 resists the ultimate torque at the lower twist as compared to all other mixes except POC80, and therefore POC40 had lower ultimate torsional toughness of 1.48 Nm/m in all mixes except POC80 of 1.14 Nm/m. The POC80 had lowest ultimate torsional toughness of 1.14 Nm/m in all mixes because POC80 resist the ultimate torsional torque at the lowest ultimate twist of 0.014 rad/m in all mixes. POC100 had minimum ultimate torque of 164.37 Nm but resisted ultimate torque at a higher twist of 0.034 rad/m compared to all replacement mixes except POC0. While the POC100 mix had higher torsional toughness of 2.48 Nm/m, which was almost equal to POC20, and two times lower than POC0 because

POC100 sustained the ultimate torque at a higher twist, except for the POC0 mix. The ultimate torsional toughness of POC0 and POC100 were higher, because both mixes resisted the ultimate torque at the higher twist, due to which, there was a larger area under the torque-twist curve. The torsional strength was also highly dependent on the splitting tensile strength of concrete and therefore the torque was reduced because of the low tensile strength of concrete caused by the substitution by POC.

All initial cracks or cracking torque of the mixes occurred in the range of 14 to 25 % of the ultimate torque. The maximum initial crack occurred at the POC100 mix, which was 25% of the ultimate torque. POC0 and POC100 had almost the same initial and ultimate twists, which means that the resistance to the initial and ultimate torque was almost similar and was at higher levels compared to other mixes. All mixes failed on ultimate torque and did not show any failure torque, because of the brittleness of concrete, which had the weakest property of both NWC and lightweight concrete (LWC). All mixes showed a sudden drop in their torque-twist curves at ultimate crack development because a failure of the concrete specimen occurred, and higher fracture energy was released.

**Table 4.3: Torsional behavior of concrete at different replacement level of POC coarse aggregate**

| Mix ID | Cracking torque | | Ultimate torque | | Initial torsional Stiffness ($kNm^2$) | Initial torsional toughness (Nm/m) | Ultimate torsional toughness (Nm/m) |
|---|---|---|---|---|---|---|---|
| | Torque (Nm) | Twist (rad/m) | Torque (Nm) | Twist (rad/m) | | | |
| POC0 | 57.46 | 0.0056 | 397.24 | 0.039 | 12.47 | 0.16 | 5.37 |
| POC20 | 51.62 | 0.0055 | 305.09 | 0.020 | 9.02 | 0.15 | 2.84 |
| POC40 | 54.77 | 0.0046 | 255.65 | 0.017 | 11.47 | 0.13 | 1.48 |
| POC60 | 47.18 | 0.0060 | 201.20 | 0.018 | 7.81 | 0.13 | 1.64 |
| POC80 | 42.61 | 0.0049 | 205.89 | 0.014 | 8.59 | 0.11 | 1.14 |
| POC100 | 41.13 | 0.0052 | 164.37 | 0.034 | 7.61 | 0.11 | 2.48 |

### 4.5.1 Acoustic emission method for crack detection

The AE method is very sensitive for the detection of initiation and propagation of cracks in concrete and can identify and detect micro-cracks induced in the concrete member or structure in the early stages (Ing et al., 2005). The analyses of AE parameters such as hits or events, energy, and signal strength are used for the detection of the initiation and propagation of the cracks in steel reinforcement members by corrosion, and also to detect early stages of corrosion (Zaki et al., 2015). From the previous study based on the test results analysis, and visual inspection of the test specimens (Shahidan et al., 2016) two parameters of AE technique – absolute energy and signal strength – are betters indicator of the damage mechanism in a concrete structure and are suited for the classification of damage in real-time under loading. Therefore, the parameters used in this study for the AE investigation of the initial and ultimate crack caused by torque are the cumulative signal strength and absolute energy parameter analysis.

#### 4.5.1.1 Absolute energy

The quantifiable measurement energy that consists of all events and AE hits is known as absolute energy (Ing et al., 2005). The torque-twist curves of the torsion machine were compared with the graphs of absolute energy to obtain the initial, and ultimate torques, and cracks, and their corresponding twists. The absolute energy graphs were used for investigating the cracking torque, and initial cracks that could not be obtained directly from the torsion machine. After applying the torque on the concrete specimen, the absolute energy did not show any response during the uncracked stage, as no fracture energy was released. After some time, the cracks were initiated inside the specimen. These small cracks, invisible to the naked eye, did not occur on the surface of the sample and could not be detected. Before the occurrence of the first crack, the intensity of AE activities was very low. When the first crack formed, there was a rise in the absolute energy graph because of energy released at higher torque. The first cracks from the absolute energy/torque-twist graph for all mixes are shown in Figure 4.10. The angles of twist for which the first crack of all mixes occurred, were in the range of 0.0046-0.0056 rad/m, which is called cracking or initial twist. Prior to this, the intensity of absolute energy was very low, because of the absence of the crack. During this time, the sudden increment in the absolute energy graph shows the occurrence of first cracks for all mixes as compared to the torque graph. While the sudden increment in the absolute energy for POC100 mixes at a cracking twist was 0.0052 rad/m, which means that increment in the absolute energy graph for POC100 mix occurred at 7.14%, 5.45%, and 13.34% of those of POC0, POC20, and POC60, respectively, before the twist. The increment in the absolute energy at the highest cracking twist was 0.0060 rad/m for POC60, while at the early cracking twist occurred for POC40. This means that POC60 show higher resistance to initial crack, but lower resistance to the initial crack by POC40 as compared to all other mixes. The rise in the absolute energy for POC20 at higher twist which was aproximatly equall to the cracking twist of the POC0 except the POC60 which resist the initial crack 8.34% less than POC60, and 5.77% higher than POC100. From the results, it can be seen that absolute energy was a good parameter for the detection and identification of the first crack in real-time, in a concrete specimen.

When the new cracks developed, the jump in the absolute energy graph was accompanied by the drop in the torque graph because of high fracture energy released due to higher crack formation. In this particular portion, the application of torque was higher than the portions, before and after the formation of a higher crack. The crack formation at higher AE activities, accompanied by the highest torque, is the ultimate crack. The specimens failed at the ultimate crack, accompanied by a drop in the torque-twist curve. The values of absolute energy for all mixes with their corresponding twists at initial and ultimate cracks are summarized in Table 4.4. As shown in Figure 4.10, the absolute energy-reduced after the initial crack is formed due to the reduction in new crack formation. Lower AE signal development caused by a further increase of torque can be attributed to the extension or propagation of the existing crack. After the first crack, micro-cracks were also observed on the surface of the concrete specimen under an applied torque. A sudden drop was observed in the torque graph after the surface crack, because of the development of the ultimate cracks, and more fracture energy was released. The angle of twist during which absolute energy suddenly increased, was in the range of 0.014-0.039 rad/m for all mixes but dropped in the torque graph after the torque was high because ultimate cracks were formed. The increase in absolute energy occurred at higher ultimate twist values of 0.039 rad/m, and 0.034 rad/m, for POC0 and POC100 mixes, respectively as compared to the other mixes. This means that both POC0 and POC100 mixes have a higher resistance to ultimate cracks because both mixes contain the same type of coarse aggregate (100% of granite, 100% of POC), which provides homogeneity of structural material. This homogeneity helps resist the torque at a higher twist. The rise in absolute energy at the lowest ultimate twist in all mixes occurred for POC40 and POC80 mixes.

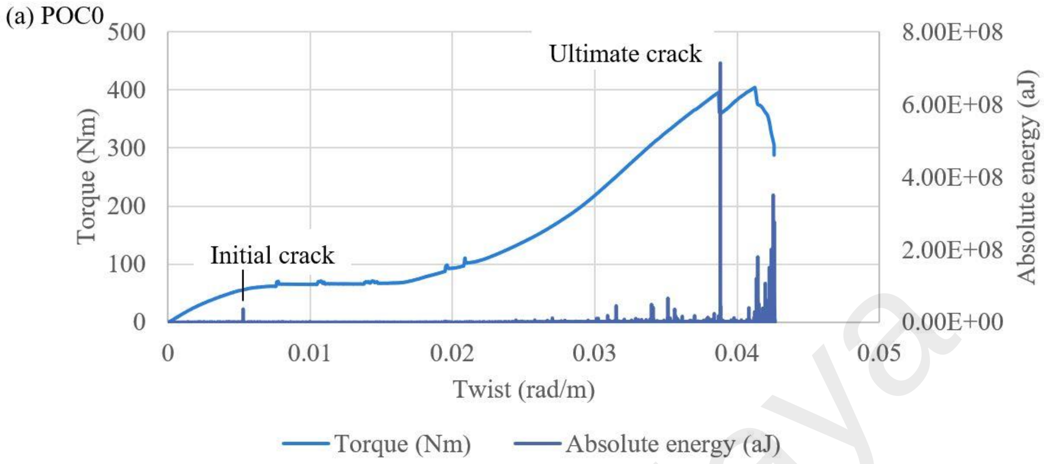


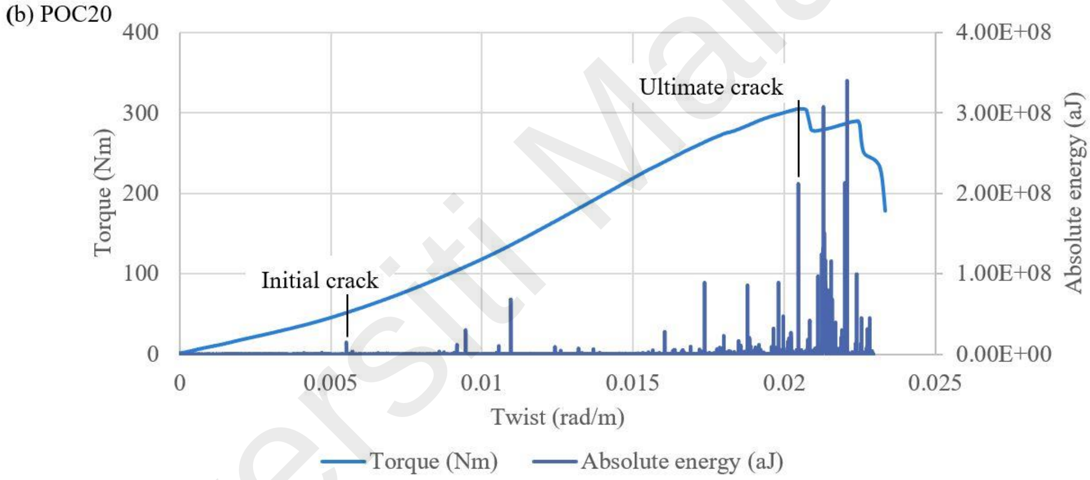


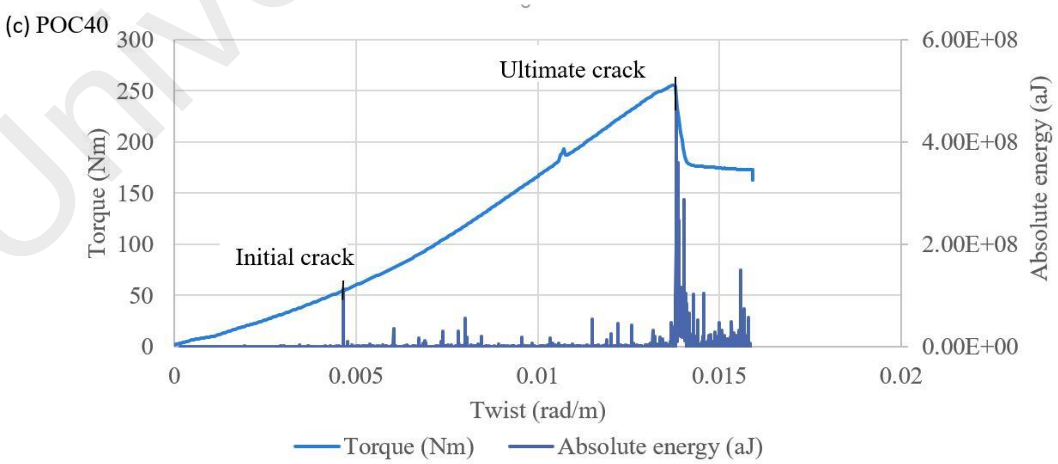

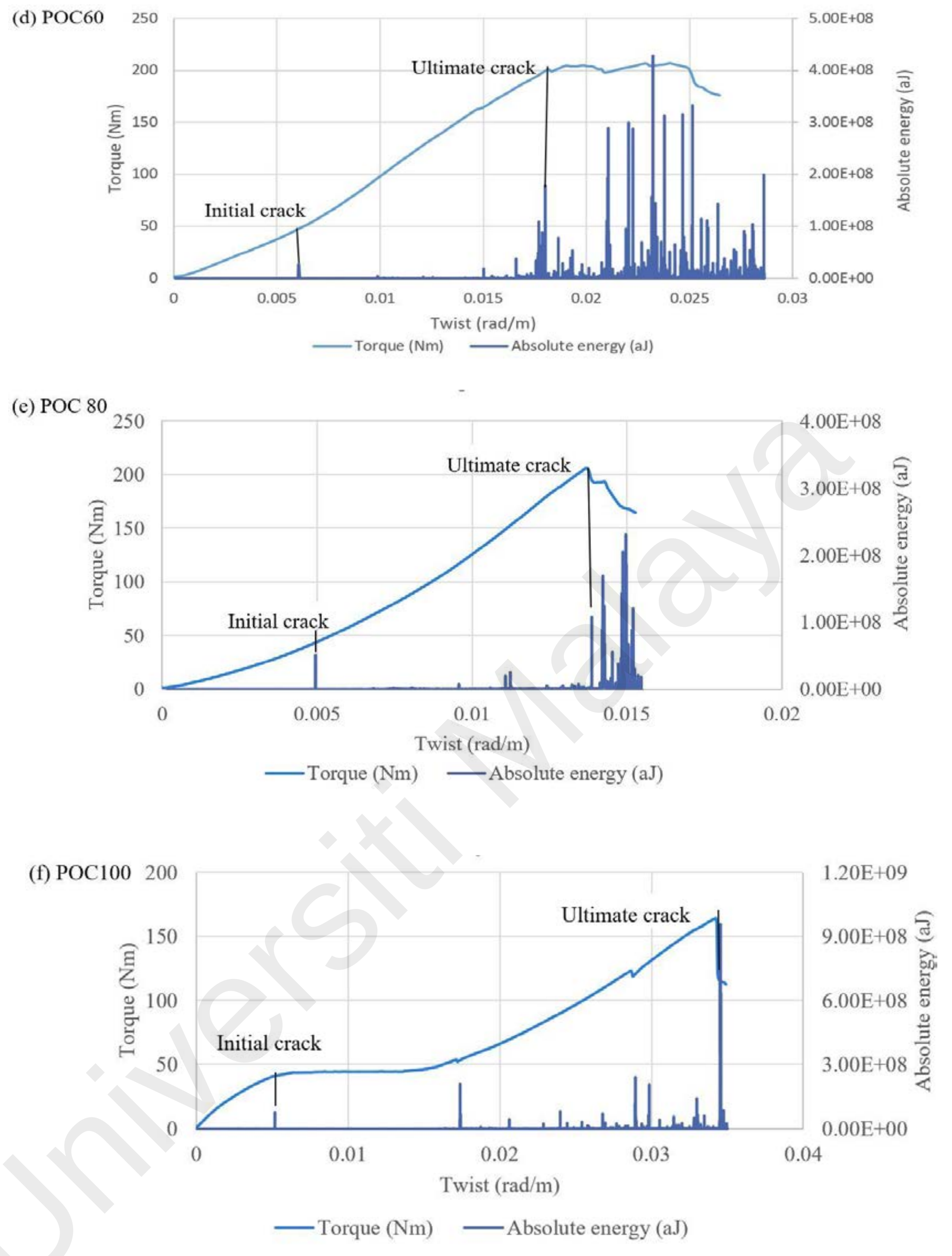


**Figure 4.10: Absolute energy and torque versus angle of twist graphs for (a) 0%, (b) 20%, (c) 40%, (d) 60%, (e) 80%, and (f) 100% replacement levels of POC.**

**Table 4.4: Initial and ultimate cracks of NWC and POC concrete.**

| Mix ID | Initial crack | | | Ultimate crack | | |
|---|---|---|---|---|---|---|
| | Absolute energy (aJ) | CSS (pVs) | Cracking twist (rad/m) | Absolute energy (aJ) | CSS (pVs) | Ultimate twist (rad/m) |
| POC0 | 3.63E+07 | 1.03E+08 | 0.0056 | 7.11E+08 | 5.44E+09 | 0.039 |
| POC20 | 1.48E+07 | 2.79E+08 | 0.0055 | 2.12E+08 | 4.71E+09 | 0.020 |
| POC40 | 1.12E+08 | 1.13E+08 | 0.0046 | 4.80E+08 | 4.69E+09 | 0.017 |
| POC60 | 2.71E +07 | 1.47E+07 | 0.0060 | 1.79E+08 | 3.90E+09 | 0.018 |
| POC80 | 5.12E+07 | 1.74E+07 | 0.0049 | 1.08E+08 | 2.26E+09 | 0.014 |
| POC100 | 7.71E+07 | 8.27E+07 | 0.0052 | 9.49E+08 | 1.26E+10 | 0.034 |

#### 4.5.1.2 Cumulative signal strength

The area covered by the voltage signal of AE throughout the waveforms is known as signal strength (Zaki et al., 2015), and the cumulative summation of signal strength is known as cumulative signal strength (CSS). The CSS/torque-twist graphs were analyzed to obtain the ultimate cracks, torque, and their corresponding twists from Figure 4.11, and it can be seen that the CSS graph did not show any response to the initial crack. During the first cracks portion, the CSS intensity was very low and did not show any response to the cracks, because CSS depends on the number of occurrences of AE events. The occurrence of AE events was low at the beginning, resulting in low CSS intensity. The AE events increased with the increase in torque, which in turn increased the intensity of CSS graphs for all mixes after approximately 50% of the torque curve.

The intensity of the CSS graph gradually increased with time under the increase of torque, because of the propagation of cracks inside the concrete. This was followed by the development of a new crack which subsequently became the largest crack of all. At this new crack development, there was a hike in the CSS graph, accompanied by rapid growth in the width of the cracks and sudden drop in the torque curve after reaching the highest torque, during when higher fracture energy was released. The same phenomenon was seen in the signal strength-time graph, which increased suddenly when the ultimate crack occurred at maximum load (Shahidan et al., 2011). This new crack is known as the ultimate crack because the torque graphs suddenly dropped after reaching the maximum value of torque accompanied by sudden jumps in the intensity of the CSS graph, compared to the loading and unloading stage (Figure 4.11). The value of CSS and their corresponding twists also decreased at ultimate cracks for all the mixes except for POC100, on increasing the amount of POC as shown in Table 4.4. POC0 and POC100 have higher values of CSS, and resisted the ultimate cracks at a higher ultimate twist of 0.039 rad/m and 0.034 rad/m, respectively, in all mixes, because both mixes contain the same type of coarse aggregate (100% of granite, 100% of POC) which provides homogeneity of structural material. This homogeneity helps resist the torque at a higher twist. The increase in the intensity of the CSS graph at the lowest ultimate twist was recorded for POC40 as shown in Figure 4.11(c). Thus, CSS is a better parameter for the detection of the growth of the crack and angle of twist at which ultimate crack developed, but is incapable of identifying the initial cracks inside the concrete specimens. The higher brittleness of NWC and POCC cannot sustain higher torque after ultimate crack, because of the absence of reinforcement.

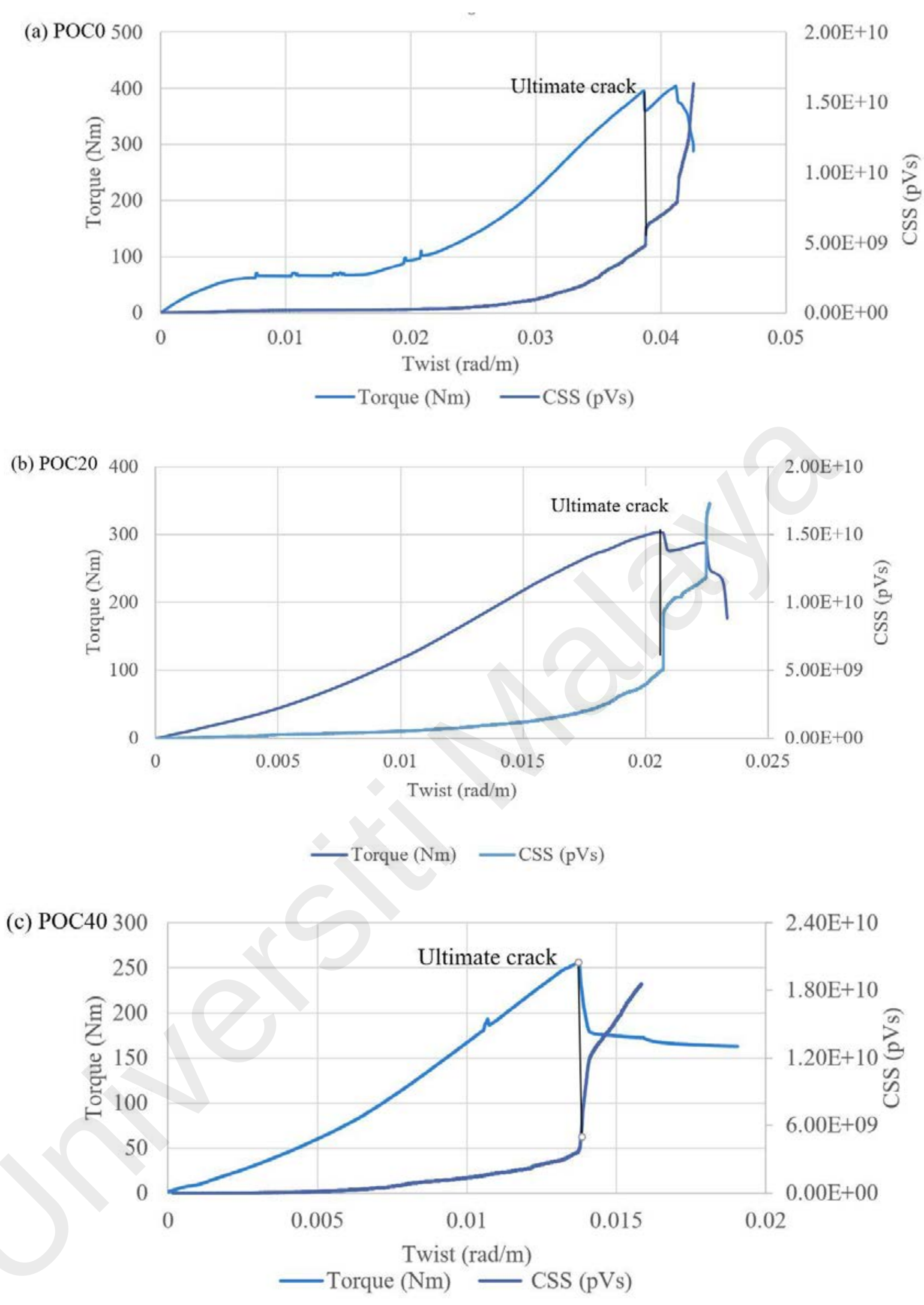
(a) POC0
Ultimate crack
Torque (Nm)
CSS (pVs)
Twist (rad/m)
Torque (Nm) CSS (pVs)
(b) POC20
Ultimate crack
Torque (Nm)
CSS (pVs)
Twist (rad/m)
Torque (Nm) CSS (pVs)
(c) POC40
Ultimate crack
Torque (Nm)
CSS (pVs)
Twist (rad/m)
Torque (Nm) CSS (pVs)

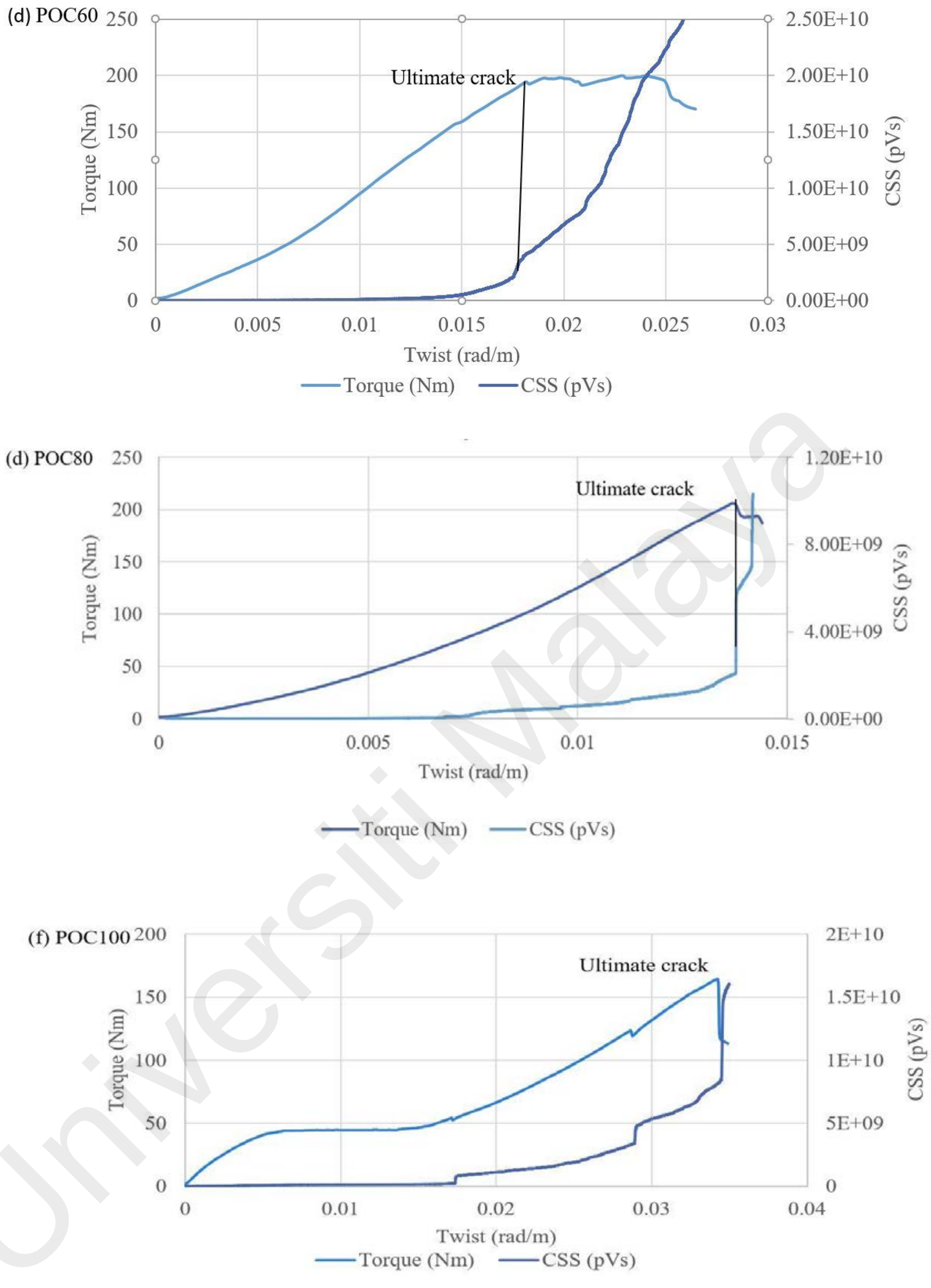


**Figure 4.11:CSS and torque versus angle of twist graphs for (a) 0 %, (b) 20%, (c) 40%, (d) 60%, (e) 80%, and (f) 100% replacement levels of POC**

### 4.5.2 Cracks

The crack mapping and crack profile of the concrete specimens at initial and ultimate cracks at various substitution levels of POC are seen in Figure 4.12. The crack width of the concrete specimens increased on increasing the substitution levels of POC. The cracks initiated from the edge of the fixed end of the torsion machine and propagated on the concrete specimen surface towards the moveable end of the torsion machine at an inclination angle of about 43-48 degrees. The failure pattern of all specimens of all mixes showed skew bending failure. Higher intensities of events were recorded upon reaching the ultimate torque caused by the failure of the concrete specimen. The ultimate crack would cause the fracture and failure of the concrete member because concrete without reinforcement is very brittle, and limited resistance to crack (George & Sofi, 2017). Higher torque cannot be withstood after the formation of the ultimate crack because of a lack of resistance by reinforcements. A sudden increase was observed in the absolute energy and CSS versus twist graphs, accompanied by a sudden drop in the torque-twist graph at the ultimate crack for all the mixes.

#### 4.5.2.1 Comparison between POC 0% and POC 100%

The initial crack of POC0 and POC100 started from 232 mm of the x-axis from the support end of the machine, and then spread on the y and z-axis as shown in Figure 4.12(a), and (f). The torque and twist at which the initial crack of POC100 occurred, were 41.12 Nm, and 0.0052 rad/m, respectively, which were 28.6%, and 7% lower than POC0, which means that the POC100 resists the initial crack or sustains the initial torque almost as much as POC0. After the first crack, the propagation of cracks was observed on the concrete specimen surface with an increase in torque. There was an increase in the intensity of events, and the crack was propagated in three dimensions to cause the ultimate crack. The ultimate crack of POC100 occurred at a twist of 0.034 rad/m and the ultimate torque was 164.37 Nm. Which was almost twice lower at a twist of 12.8% lower, than the POC0 mix. The higher intensities of events were recorded at ultimate cracks for both mixes because both mixes contain the same type of coarse aggregate (100% of granite, 100% of POC) which provides homogeneity of structural material. This homogeneity helps resist the torque at a higher twist. In addition, higher fracture energy was released for both mixes. The crack mapping of the initial and ultimate cracks and images of the concrete specimen shows that the POC100 specimen broke into two large pieces without breaking into small pieces, while POC0 showed a small crack opening on the surface. The ultimate crack of both mixes occurred suddenly, and the samples did not resist the torque after the ultimate crack.

#### 4.5.2.2 Comparison between the mixes

The cracking torque of concrete reduced on increasing the substitution levels of POC. The range of cracking torque was between 41.13-57.46 Nm, and their angles of a twist at which mixes resisted the initial crack were in the range of 0.0046-0.0056 rad/m. In all mixes, the POC60 showed the highest resistance to the initial crack, and the twist at which the initial crack occurred was 0.0060 rad/m. It is also seen from Figure 4.12(d), that the initial crack of POC60 started at a higher position, i.e., at 242 mm and 21mm on the x-axis, and y-axis, respectively, as compared to all other mixes. POC40 resisted the initial crack at the lowest twist of 0.0046 rad/m but sustained higher torque of 54.77 Nm compared to all other mixes, except the POC0. POC40 also had higher initial torsional stiffness of 11.47 $kNm^2$, compared to all other mixes except POC0, while POC80 had a higher initial torsional stiffness of 8.59 $kNm^2$ compared to POC60, and POC100, because POC80 sustained initial torque at a lower angle of twist (except POC40) (Table 4.4). The initial torsional toughness for all the mixes reduced on increasing the amount of the POC, because of the lower area under the torsional-twist curve for all mixes, and occurrence of the initial cracks for all mixes almost at a similar cracking twist.

After some time of the initial crack, the cracks were seen and propagated on the surface of concrete specimens accompanied by an increase in the AE activities in all directions (Figure 4.12). The width of the ultimate crack up to POC60 was increased gradually, and the specimen did not split into parts. The crack width of POC80 and POC100 specimens increased drastically, and the samples split into two, and three parts, respectively, but were not broken into smaller pieces. The resistance to ultimate crack for all the mixes decreased on increasing the substitution levels of POC, except for POC100, and the angle of twist at which ultimate cracks occurred for all mixes was in the range of 0.14-0.39 rad/m as shown in Table 4.4. POC40 and POC80 had minimum resistance to the ultimate crack, which occurred at the minimum ultimate twist of 0.017 rad/m and 0.014 rad/m, respectively. Low intensities of events were recorded for the POC40, and POC80 as shown in Figure 4.12(c), and (e). The expansion of the ultimate cracks, as seen in crack mapping, was approximately 258 mm, 70 mm, and 1 mm on x, y, and z-axis for all mixes, and higher intensities of events were recorded for the POC0 and POC100 compared to all other mixes (Figure 4.12). The ultimate torsional toughness values of all mixes also reduced with an increase in the incorporation of POC, except for POC100; the resistance to the ultimate crack decreased on increasing the substitution of POC.

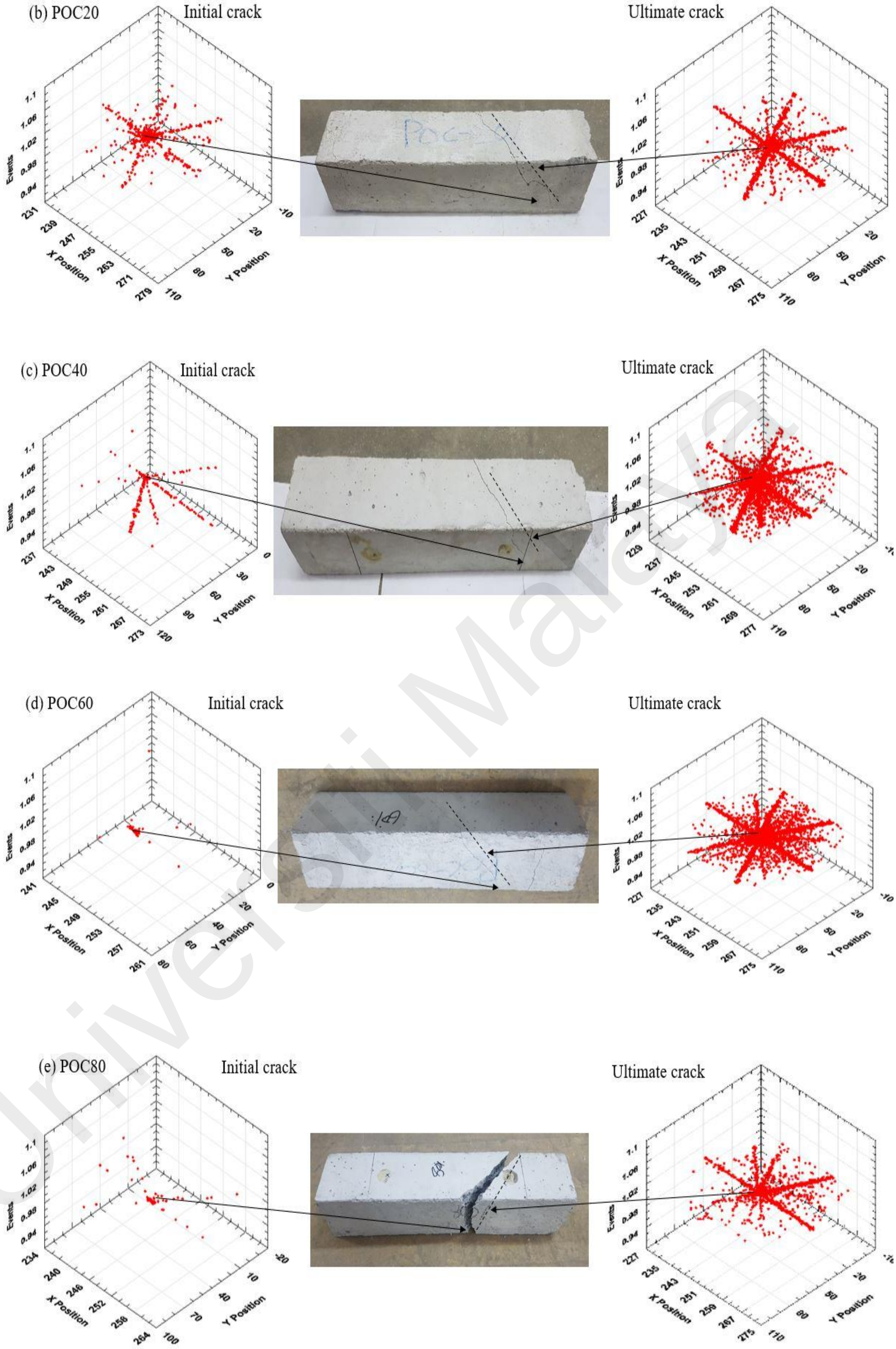
(b) POC20
Initial crack
Ultimate crack
(c) POC40
Initial crack
Ultimate crack
(d) POC60
Initial crack
Ultimate crack
(e) POC80
Initial crack
Ultimate crack
Events
X Position
Y Position


**Figure 4.12: Crack mapping, and profile of initial cracks, concrete specimen, and ultimate cracks for (a) 0 %, (b) 20%, (c) 40%, (d) 60%, (e) 80%, and (f) 100% replacement levels of POC**

# CHAPTER 5: CONCLUSIONS AND RECOMMENDATIONS

## 5.1 Conclusions

The following conclusions were drawn based on experimental test results.

The loose and compacted bulk densities of POC had 599.991 $Kg/m^3$, and 694.37 $Kg/m^3$ which had 41.90 %, and 44.17 % lower than granite, respectively. The value of specific gravity in oven-dried condition and SSD condition of POC had 1.4 and 1.54 while 2.59 and 2.6 for granite, respectively. The water absorption of POC was 9.38% which is 23.475 times higher than granite while 0.4% for the granite. The AIV value of POC was 47.88% which is 2.34 times higher than the AIV of granite of 20.47%.

The maximum reduction in hard density, compression strength, splitting tensile strength, and flexural strength of concrete of 18.83%, 37.25%, 30.94%, and 14.31%, respectively were occurred at the full substitution level of POC. Meanwhile, the water absorption of the POC100 mix was 1.78 times higher than the control mix. The impact energies at first and failure crack at the full substitution of POC were approximately 1.60 times higher than the control mix.

The initial and ultimate torque was reduced while initial and ultimate cracks were increased by increasing the substitution level of POC. The POC0 and POC100 have the almost same resistance to initial and ultimate torque while the initial torsional stiffness and ultimate torsional toughness had almost 1.64 and 2 times lower than the control mix. POC40 had a maximum initial torsional stiffness but the lowest angle of twist in all the mixes.

The absolute energy is a useful AE parameter for the detection of both initial and ultimate torsional cracks while the CSS parameter is capable to identify the growth of the crack and the ultimate torsional crack. The higher intensity of the AE event recorded and higher energy dissipation occurred for POC0 and POC100 mixes. The initial crack for all mixes has occurred almost in the range of 14-25% of the ultimate crack. The width of the crack of specimens was increased by increasing the substitution levels of POC. The POC80 and POC100 were broken into two and three pieces respectively but still not into small pieces.

## 5.2 Recommendations for future study

The study on the torsional behaviours, and the location of torsional cracks concrete based on LWA especially POC coarse aggregate based concrete is very limited. POC concrete is still of great interest, and further research can be carried out to gaing of full confidence. The following important recommendations for future study.

- Further work can be carried on replacing the natural fine aggregates with POC fine aggregates at different replacement levels, which is for economical, social and environmental benefits. To investigate the torsional behaviours and location of torsional crack of concrete by using the parameters of AE method by replacing the sand with POC fine aggregates.
- To improve the ductility characteristics of POC concrete by adding of polymers (crumb rubber or recycled plastics) by replacing of both natural coarse and fine aggregates with different coarse and fine POC aggregates replacements.

## REFERENCES


Abutaha, F., Abdul Razak, H., & Ibrahim, H. A. (2017). Effect of coating palm oil clinker aggregate on the engineering properties of normal grade concrete. *Coatings, 7*(4), 175.

Abutaha, F., Razak, H. A., Ibrahim, H. A., & Ghayeb, H. H. (2018). Adopting particle-packing method to develop high strength palm oil clinker concrete. *Resources, conservation and Recycling, 131*, 247-258.

Abutaha, F., Razak, H. A., & Kanadasan, J. (2016). Effect of palm oil clinker (POC) aggregates on fresh and hardened properties of concrete. *Construction and Building Materials, 112*, 416-423.

ACI. (2002). Measurement of Properties of Fiber Reinforced Concrete *ACI 544.2R-89*: American Concrete Institute

Ahmad, H., Hilton, M., Mohd, S., & Mohd Noor, N. (2007). Mechanical properties of palm oil clinker concrete.

Ahmmad, R., Alengaram, U. J., Jumaat, M. Z., Sulong, N. R., Yusuf, M. O., & Rehman, M. A. (2017). Feasibility study on the use of high volume palm oil clinker waste in environmental friendly lightweight concrete. *Construction and Building Materials, 135*, 94-103.

Ahmmad, R., Jumaat, M., Bahri, S., & Islam, A. S. (2014). Ductility performance of lightweight concrete element containing massive palm shell clinker. *Construction and Building Materials, 63*, 234-241.

Ahmmad, R., Jumaat, M. Z., Alengaram, U. J., Bahri, S., Rehman, M. A., & bin Hashim, H. (2016). Performance evaluation of palm oil clinker as coarse aggregate in high strength lightweight concrete. *Journal of Cleaner Production, 112*, 566-574.

Alengaram, U. J., Al Muhit, B. A., & bin Jumaat, M. Z. (2013). Utilization of oil palm kernel shell as lightweight aggregate in concrete–A review. *Construction and Building Materials, 38*, 161-172.

Alsubari, B., Shafigh, P., Ibrahim, Z., Alnahhal, M. F., & Jumaat, M. Z. (2018). Properties of eco-friendly self-compacting concrete containing modified treated palm oil fuel ash. *Construction and Building Materials, 158*, 742-754.

Aslam, M., Shafigh, P., & Jumaat, M. Z. (2016). Oil-palm by-products as lightweight aggregate in concrete mixture: a review. *Journal of Cleaner Production, 126*, 56-73.

Aslam, M., Shafigh, P., & Jumaat, M. Z. (2017). High strength lightweight aggregate concrete using blended coarse lightweight aggregate origin from palm oil industry. *Sains Malaysiana, 46*(4), 667-675.

Aslam, M., Shafigh, P., Jumaat, M. Z., & Lachemi, M. (2016). Benefits of using blended waste coarse lightweight aggregates in structural lightweight aggregate concrete. *Journal of Cleaner Production, 119*, 108-117.

Aslam, M., Shafigh, P., Nomeli, M. A., & Jumaat, M. Z. (2017). Manufacturing of high-strength lightweight aggregate concrete using blended coarse lightweight aggregates. *Journal of Building Engineering, 13*, 53-62.

ASTM C127 - 15. (2015). Standard test method for relative density (specific gravity) and absorption of coarse aggregate. West Conshohocken, PA, USA: American Society for Testing and Materials.

BS EN 206:2013. (2014). Concrete — Specification, performance, production, and conformity.

BS EN 1097-2:1998. (1998). Testing aggregates. Method for determination of aggregate impact value (AIV). London: British Standards Institution.

BS EN 1097-3:1998. (1998). Tests for mechanical and physical properties of aggregates. Determination of loose bulk density and voids. London: British Standards Institution.

BS EN 12390-2:2019. (2019). Testing hardened concrete. Making and curing specimens for strength tests. London: British Standards Institution.

BS EN 12390-3:2019. (2019). Testing hardened concrete. Compressive strength of test specimens. London: British Standards Institution.

BS EN 12390-5:2019. (2019). Testing hardened concrete. Flexural strength of test specimens. London: British Standards Institution.

BS EN 12390-6:2009. (2010). Testing hardened concrete. Tensile splitting strength of test specimens. London: British Standards Institution.

Cao, X., Wu, L., & Li, Z. (2019). Behaviour of steel-reinforced concrete columns under combined torsion based on ABAQUS FEA. *Engineering Structures*, 109980.

Düzgün, O. A., Gül, R., & Aydin, A. C. (2005). Effect of steel fibers on the mechanical properties of natural lightweight aggregate concrete. *Materials Letters, 59*(27), 3357-3363.

Ebrahimian, Z., Ahmadi, M., Sadri, S., Li, B., & Moradian, O. (2019). Wavelet analysis of acoustic emissions associated with cracking in rocks. *Engineering Fracture Mechanics, 217*, 106516.

Fuad Abutaha, Hashim Abdul Razak, & Kanadasan, J. (2016). Effect of palm oil clinker (POC) aggregates on fresh and hardened properties of concrete. *Construction and Building Materials, 112*, 416–423.

Gayana, B., & Chandar, K. R. (2018). Sustainable use of mine waste and tailings with suitable admixture as aggregates in concrete pavements-A review. *Advances in concrete construction, 6*(3), 221-243.

George, A., & Sofi, A. (2017). Torsional strengthening of normal weight concrete and light weight concrete using steel fibres. *Materials Today: Proceedings, 4*(9), 9846-9850.

George, A., & Sofi, A. (2018). Torsional and cracking behaviours of normal weight and coconut shell lightweight concretes. *Journal of Engineering Science and Technology, 13*, 4104-4117.

Gunasekaran, K., Annadurai, R., & Kumar, P. (2013). Plastic shrinkage and deflection characteristics of coconut shell concrete slab. *Construction and Building Materials, 43*, 203-207.

Gunasekaran, K., Ramasubramani, R., Annadurai, R., & Chandar, S. P. (2014). Study on reinforced lightweight coconut shell concrete beam behavior under torsion. *Materials & Design, 57*, 374-382.

Halicka, A., Ogrodnik, P., & Zegardlo, B. (2013). Using ceramic sanitary ware waste as concrete aggregate. *Construction and Building Materials, 48*, 295-305.

Hamada, H. M., Jokhio, G. A., Al-Attar, A. A., Yahaya, F. M., Muthusamy, K., Humada, A. M., & Gul, Y. (2019). The use of palm oil clinker as a sustainable construction material: A review. *Cement and Concrete Composites, 106*, 103447.

Hamada, H. M., Yahaya, F. M., Muthusamy, K., Jokhio, G. A., & Humada, A. M. (2019). Fresh and hardened properties of palm oil clinker lightweight aggregate concrete incorporating nano-palm oil fuel ash. *Construction and Building Materials, 214*, 344-354.

Haque, M., Al-Khaiat, H., & Kayali, O. (2004). Strength and durability of lightweight concrete. *Cement and Concrete Composites, 26*(4), 307-314.

Huda, M. N., Jumaat, M. Z., Islam, A., Obaydullah, M., & Hosen, M. A. (2017). Palm oil industry's bi-products as coarse aggregate in structural lightweight concrete. *Computers and Concrete, 19*(5), 515-526.

Hwang, C.-L., Bui, L. A.-T., Lin, K.-L., & Lo, C.-T. (2012). Manufacture and performance of lightweight aggregate from municipal solid waste incinerator fly ash and reservoir sediment for self-consolidating lightweight concrete. *Cement and Concrete Composites, 34*(10), 1159-1166.

Ibrahim, H. A., & Razak, H. A. (2016). Effect of palm oil clinker incorporation on properties of pervious concrete. *Construction and Building Materials, 115*(4), 70-77.

Ibrahim, H. A., Razak, H. A., & Abutaha, F. (2017). Strength and abrasion resistance of palm oil clinker pervious concrete under different curing method. *Construction and Building Materials, 147*, 576-587.

Ing, M., Austin, S., & Lyons, R. (2005). Cover zone properties influencing acoustic emission due to corrosion. *Cement and Concrete Research, 35*(2), 284-295.

Islam, A., Alengaram, U. J., Jumaat, M. Z., Ghazali, N. B., Yusoff, S., & Bashar, I. I. (2017). Influence of steel fibers on the mechanical properties and impact resistance of lightweight geopolymer concrete. *Construction and Building Materials, 152*, 964-977.

Ismail, M. K., & Hassan, A. A. (2019). Abrasion and impact resistance of concrete before and after exposure to freezing and thawing cycles. *Construction and Building Materials, 215*, 849-861.

Jumaat, M. Z., Alengaram, U. J., Ahmmad, R., Bahri, S., & Islam, A. S. (2015). Characteristics of palm oil clinker as replacement for oil palm shell in lightweight concrete subjected to elevated temperature. *Construction and Building Materials, 101*, 942-951.

Jumaat, M. Z., Alengaram, U. J., & Mahmud, H. (2009). Shear strength of oil palm shell foamed concrete beams. *Materials & Design, 30*(6), 2227-2236.

Kabir, S. A., Alengaram, U. J., Jumaat, M. Z., Yusoff, S., Sharmin, A., & Bashar, I. I. (2017). Performance evaluation and some durability characteristics of environmental friendly palm oil clinker based geopolymer concrete. *Journal of Cleaner Production, 161*, 477-492.

Kanadasan, J., & Razak, H. A. (2014). Mix design for self-compacting palm oil clinker concrete based on particle packing. *Materials & Design (1980-2015), 56*, 9-19.

Kanadasan, J., & Razak, H. A. (2015). Engineering and sustainability performance of self-compacting palm oil mill incinerated waste concrete. *Journal of Cleaner Production, 89*, 78-86.

Karim, M. R., Chowdhury, F. I., Zabed, H., & Saidur, M. (2018). Effect of elevated temperatures on compressive strength and microstructure of cement paste containing palm oil clinker powder. *Construction and Building Materials, 183*, 376-383.

Khankhaje, E., Salim, M. R., Mirza, J., Hussin, M. W., & Rafieizonooz, M. (2016). Properties of sustainable lightweight pervious concrete containing oil palm kernel shell as coarse aggregate. *Construction and Building Materials, 126*, 1054-1065.

Kockal, N. U., & Ozturan, T. (2011). Strength and elastic properties of structural lightweight concretes. *Materials & Design, 32*(4), 2396-2403.

Landis, E. N., & Baillon, L. (2002). Experiments to relate acoustic emission energy to fracture energy of concrete. *Journal of Engineering Mechanics, 128*, 698-702.

Mannan, M., & Ganapathy, C. (2004). Concrete from an agricultural waste-oil palm shell (OPS). *Building and Environment, 39*(4), 441-448.

Mannan, M. A., & Ganapathy, C. (2002). Engineering properties of concrete with oil palm shell as coarse aggregate. *Construction and Building Materials, 16*(1), 29-34.

Mazal, P., Vlasic, F., & Koula, V. (2015). Use of acoustic emission method for identification of fatigue micro-cracks creation. *Procedia Engineering, 133*, 379-388.

Mo, K. H., Yap, S. P., Alengaram, U. J., Jumaat, M. Z., & Bu, C. H. (2014). Impact resistance of hybrid fibre-reinforced oil palm shell concrete. *Construction and Building Materials, 50*, 499-507.

Mohammadhosseini, H., Tahir, M. M., & Sam, A. R. M. (2018). The feasibility of improving impact resistance and strength properties of sustainable concrete composites by adding waste metalized plastic fibres. *Construction and Building Materials, 169*, 223-236.

Mohammed, B. S., Al-Ganad, M. A., & Abdullahi, M. (2011). Analytical and experimental studies on composite slabs utilising palm oil clinker concrete. *Construction and Building Materials, 25*(8), 3550-3560.

Mohammed, B. S., Foo, W., & Abdullahi, M. (2014). Flexural strength of palm oil clinker concrete beams. *Materials & Design, 53*, 325-331.

Mohammed, B. S., Foo, W., Hossain, K., & Abdullahi, M. (2013). Shear strength of palm oil clinker concrete beams. *Materials & Design, 46*, 270-276.

MS 522: PART 1:2003. (2003). Portland Cement (ordinary and rapid-hardening). Malaysia

Nair, A., & Cai, C. (2010). Acoustic emission monitoring of bridges: Review and case studies. *Engineering Structures, 32*(6), 1704-1714.

Nayaka, R. R., Alengaram, U. J., Jumaat, M. Z., Yusoff, S. B., & Ganasan, R. (2019). Performance evaluation of masonry grout containing high volume of palm oil industry by-products. *Journal of Cleaner Production, 220*, 1202-1214.

Nazreen, M. S., Mohamed, R. N., Ab Kadir, M. A., Azillah, N., Shukri, N. A., Mansor, S., & Zamri, F. (2018). *Characterization of lightweight concrete made of palm oil clinker aggregates.* Paper presented at the MATEC Web of Conferences.

Noorsuhada M.N, Soffian Noor M.S, Muhammad Zakaria M, Azmi, Jalilluddin A.M, Aqil, . . . A.G., K. D. (2017). *Structural health monitoring of reinforced concrete beam-column joint using acoustic emission technique*. Paper presented at the Proceedings of 71st ISERD International Conference., Brisbane, Australia.

Okay, F., & Engin, S. (2012). Torsional behavior of steel fiber reinforced concrete beams. *Construction and Building Materials, 28*(1), 269-275.

Omar, A. T., & Hassan, A. A. (2019). Use of polymeric fibers to improve the mechanical properties and impact resistance of lightweight SCC. *Construction and Building Materials, 229*, 116944.

Poongodi, K., & Murthi, P. (2020). Impact strength enhancement of banana fibre reinforced lightweight self-compacting concrete. *Materials Today: Proceedings*.

Qian, Y., Farnam, Y., & Weiss, J. (2014). Using acoustic emission to quantify freeze–thaw damage of mortar saturated with NaCl solutions.

Rahal, K. N. (2013). Torsional strength of normal and high strength reinforced concrete beams. *Engineering Structures, 56*, 2206-2216.

Rao, T. G., & Seshu, D. R. (2003). Torsion of steel fiber reinforced concrete members. *Cement and Concrete Research, 33*(11), 1783-1788.

Rao, T. G., & Seshu, D. R. (2006). Torsional response of fibrous reinforced concrete members: Effect of single type of reinforcement. *Construction and Building Materials, 20*(3), 187-192.

Shafigh, P., Mahmud, H. B., & Jumaat, M. Z. (2012). Oil palm shell lightweight concrete as a ductile material. *Materials & Design (1980-2015), 36*, 650-654.

Shahidan, S., Abdullah, S. R., & Ismail, I. (2016). Relationship between AE signal strength and absolute energy in determining damage classification of concrete structures. *Jurnal Teknologi, 78*, 91-98.

Shahidan, S., Md Nor, N., Ibrahim, A., Muhamad Bunnori, N., Saliah, M., & Noor, S. (2011). Relationship between acoustic emission signal strength and damage evaluation of reinforced concrete structure: Case studies.

Sharath, S., Gayana, B., Reddy, K. R., & Chandar, K. R. (2019). Experimental investigations on performance of concrete incorporating Precious Slag Balls (PS Balls) as fine aggregates. *Advances in concrete construction, 8*(3), 239-246.

Shardakov, I., Shestakov, A., & Glot, I. (2018). Elastic and Dissipative Properties of Concrete under Impact Loads. *Procedia Structural Integrity, 9*, 199-206.

Siddique, S., Shrivastava, S., Chaudhary, S., & Gupta, T. (2018). Strength and impact resistance properties of concrete containing fine bone china ceramic aggregate. *Construction and Building Materials, 169*, 289-298.

Suman, S., & Rajasekaran, C. (2016). Mechanical properties of recycled aggregate concrete produced with Portland Pozzolana Cement. *Advances in concrete construction, 4*(1), 27-35.

Świt, G. (2018). Acoustic emission method for locating and identifying active destructive processes in operating facilities. *Applied Sciences, 8*(8), 1295.

Thomas, J., Thaickavil, N. N., & Abraham, M. P. (2018). Copper or ferrous slag as substitutes for fine aggregates in concrete. *Advances in Concrete Construction,, 6*(5), 545-560.

Topçu, İ. B., & Uygunoğlu, T. (2010). Effect of aggregate type on properties of hardened self-consolidating lightweight concrete (SCLC). *Construction and Building Materials, 24*(7), 1286-1295.

Wang, X., Liu, B., & Zhang, C. (2016). Seismic behavior of recycled aggregate concrete beams under cyclic torsion. *Construction and Building Materials, 129*, 193-203.

Yan, K., Xu, H., Shen, G., & Liu, P. (2013). Prediction of splitting tensile strength from cylinder compressive strength of concrete by support vector machine. *Advances in Materials Science and Engineering, 2013*.

Yap, S. P., Alengaram, U. J., Jumaat, M. Z., & Khaw, K. R. (2015). Torsional behaviour of steel fibre-reinforced oil palm shell concrete beams. *Materials & Design, 87*, 854-862.

Yap, S. P., Alengaram, U. J., Jumaat, M. Z., & Khaw, K. R. (2016). Torsional and cracking characteristics of steel fiber-reinforced oil palm shell lightweight concrete. *Journal of Composite Materials, 50*(1), 115-128.

Yap, S. P., Bu, C. H., Alengaram, U. J., Mo, K. H., & Jumaat, M. Z. (2014). Flexural toughness characteristics of steel–polypropylene hybrid fibre-reinforced oil palm shell concrete. *Materials & Design, 57*, 652-659.

Yap, S. P., Khaw, K. R., Alengaram, U. J., & Jumaat, M. Z. (2015). Effect of fibre aspect ratio on the torsional behaviour of steel fibre-reinforced normal weight concrete and lightweight concrete. *Engineering Structures, 101*, 24-33.

Yew, M. K., Othman, I., Yew, M. C., Yeo, S., & Mahmud, H. (2011). Strength properties of hybrid nylon-steel and polypropylene-steel fibre-reinforced high strength concrete at low volume fraction. *International Journal of Physical Sciences, 6*(33), 7584-7588.

Yoo, D.-Y., & Banthia, N. (2019). Impact resistance of fiber-reinforced concrete–A review. *Cement and Concrete Composites, 104*, 103389.

Zaki, A., Chai, H. K., Aggelis, D. G., & Alver, N. (2015). Non-destructive evaluation for corrosion monitoring in concrete: A review and capability of acoustic emission technique. *Sensors, 15*(8), 19069-19101.

Zhang, M., Shim, V., Lu, G., & Chew, C. (2005). Resistance of high-strength concrete to projectile impact. *International Journal of Impact Engineering, 31*(7), 825-841.

# LIST OF PUBLICATION

Khan, S.; Yap, S.P.; Tan, C.G.; Ganasan, R.; Sherif, M.M.; El-Shafie, A. Torsional Crack Localization in Palm Oil Clinker Concrete Using Acoustic Emission Method. *Materials* **2021**, *14*, 5446. https://doi.org/10.3390/ma14185446.